

**FABRICATION SiO_2 -NiO FOAM *via* REPLICATION TECHNIQUE FOR
STEAM METHANE REFORMING CATALYST AT LOW TEMPERATURES**

RIZAMARHAIZA BINTI MUDA



UNIVERSITI TUN HUSSEIN ONN MALAYSIA

UNIVERSITI TUN HUSSEIN ONN MALAYSIA

STATUS CONFIRMATION FOR THESIS DOCTOR OF PHILOSOPHY

FABRICATION SiO₂-NiO FOAM *via* REPLICATION TECHNIQUE FOR
STEAM METHANE REFORMING CATALYST AT LOW TEMPERATURES

ACADEMIC SESSION: 2021/2022

I, **Rizamarhaiza binti Muda**, agree to allow this Doctoral Thesis to be kept at the Library under the following terms:

1. This Thesis is the property of the Universiti Tun Hussein Onn Malaysia.
2. The library has the right to make copies for educational purposes only.
3. The library is allowed to make copies of this report for educational exchange between higher educational institutions.
4. The library is allowed to make available full text access of the digital copy via the internet by Universiti Tun Hussein Onn Malaysia in downloadable format provided that the Thesis is not subject to an embargo. Should an embargo be in place, the digital copy will only be made available as set out above once the embargo has expired.
5. ** Please Mark (v)



CONFIDENTIAL

(Contains information of high security or of great importance to Malaysia as STIPULATED under the OFFICIAL SECRET ACT 1972) *Title and Abstract only*



RESTRICTED

(Contains restricted information as determined by the Organization/institution where research was conducted)-
Title, Abstract and Introduction only



EMBARGO

_____ until _____
(date) (date)



FREE ACCESS

Approved by,

(WRITER'S SIGNATURE)

(SUPERVISOR'S SIGNATURE)

Permanent Address:

NO, 81 RUMAH AWAM KOS RENDAH,
KAMPUNG RAJA, 22200 BESUT,
TERENGGANU

Date : 18/04/2021

Date: 18/04/2021

NOTE:

** If this Doctoral Thesis classified as CONFIDENTIAL or RESTRICTED, please attach the letter from the relevant authority/organization stating reasons and duration for such classification

This thesis has been examined on date 18/11/2020 and is sufficient in fulfilling the scope and quality for the purpose of awarding the Doctor of Philosophy in Mechanical Engineering.

Chairperson:

ASSOC. PROF. IR. TS. DR AL EMRAN BIN ISMAIL
Faculty of Mechanical and Manufacturing Engineering
Universiti Tun Hussein Onn Malaysia

Examiners :

PROF DR. MOHD MUSTAFA AL BAKRI BIN ABDULLAH
Faculty Engineering Technology (FETech)
Universiti Malaysia Perlis

ASSOC PROF TS. DR HAMIMAH BINTI ABD RAHMAN
Faculty of Mechanical and Manufacturing Engineering
Universiti Tun Hussein Onn Malaysia

FABRICATION SiO_2 -NiO FOAM *via* REPLICATION TECHNIQUE FOR STEAM
METHANE REFORMING CATALYST AT LOW TEMPERATURES

RIZAMARHAIZA BINTI MUDA

A thesis submitted in
fulfillment of the requirement for the award of the
Doctor of Philosophy in Mechanical Engineering



Faculty of Mechanical and Manufacturing Engineering
Universiti Tun Hussein Onn Malaysia

MARCH 2021

I hereby declare that the work in this thesis is my own except for quotations and summaries which have been duly acknowledged

Student :. -----

RIZAMARHAIZA BINTI MUDA

Date : 18/04/2021

Supervisor : -----

PROF MADYA DR HARIATI BINTI

MOHD TAIB@TAIB

Co-Supervisor : -----

PROF MADYA DR SUFIZAR BINTI AHMAD

Co-Supervisor : -----

PROF MADYA DR MAS FAWZI BIN MOHD ALI



PTT AUTHM
PERPUSTAKAAN TUNKU TUN AMINAH

To my precious Allah SWT, who gave me a new life, hope and purpose of life.

To my beloved Prophet Muhammad S.A.W who gave me guidance thru his sunnah and hadis.

To Abah, Mak and my in-laws, who giving all they have.

To my beloved husband, Mohd Firdaus bin Zulkifli, who supported me each step of the way,

And to my beloved daughters, Nur Raisha Sofia and Nur Rania Sakina who are my inspiration and motivation in completing this thesis

ACKNOWLEDGEMENT

Firstly, I thank Allah SWT for his grace and strength given to me so that this research could be made possible. Secondly, I would like to extend my gratitude to my supervisor, Associate Prof Dr Hariati Taib and co-supervisor, Associate Prof Dr Sufizar Ahmad and Associate Prof Dr Mas Fawzi Mohd Ali for their continuous understanding, encouragement and trust in me throughout the entire research. I am grateful for the endless construction comments and careful review of all the report.

I would also like to thank the following, who have helped me in various ways:

- Ministry of higher education Malaysia for research financial support under a FRGS Grant (1593).Moreover, for the MyBrain15 Scholarship (MyPhD) program for my studies scholarships.
- University Tun Hussein Onn Malaysia especially Research Management Centre (RMC) for their financial support for paper publication and conference fees.
- Faculty of Mechanical and Manufacturing Engineering and material engineering and design department members, for their understanding and the facilities support in accomplishing this resear



ABSTRACT

Porous ceramic is a type of material that has highly open and partially interconnected pores. It has a wide range of applications, which include catalyst support, filtration, adsorption and separation. The aim of this study is to fabricate Silica-Nickel Oxide ($\text{SiO}_2\text{-NiO}$) foams in the range 70 μm to 150 μm open pore size, 75% to 90% of porosity, good physical and mechanical properties as a criteria catalyst in the Steam Methane Reforming (SMR) application. In this work, the porous foam fabricated with different compositions of SiO_2 as derived from Rice Husk Ash (RHA) (20% to 35%) and at different sintering temperatures (850°C to 1250°C) by using replication sponge method. Characterisation of SiO_2 and $\text{SiO}_2\text{-NiO}$ foams included morphological analysis, porosity and density test, and compression test as criteria compatibility of SiO_2 and NiO as a catalyst in methane reforming. The morphology result showed open pores with size ranging from 15.13 μm to 76.06 μm . The lowest result for apparent porosity obtained was 65% and the highest was 81.74%, while the lowest and highest values for bulk density were 0.626 g/cm^3 and 1.070 g/cm^3 , respectively. The result for compressive strength was within the range of 0.06 MPa to 0.47 MPa. Throughout the observations, the maximum performance shown the $\text{SiO}_2\text{-NiO}$ foam produced with 35wt% SiO_2 and 5wt% NiO was found to have mechanical and physical properties much like those of a filter catalyst in SMR. The methane (CH_4) conversion using the $\text{SiO}_2\text{-NiO}$ foam was shown the range of 34.72% to 42.6% at different low temperatures. The results proved that the foam from silica as derived from RHA and NiO is very suitable to be used as a catalyst in SMR due to achieved the minimum CH_4 conversion over than 21%.

ABSTRAK

Seramik berliang adalah sejenis bahan yang mempunyai liang yang sangat terbuka dan saling bergabung antara satu sama lain. Ia mempunyai pelbagai aplikasi termasuklah sebagai sokongan pemangkin, penapisan, penjerapan, dan pemisahan. Tujuan kajian ini dilakukan adalah untuk menghasilkan busa Silika-Nikel oksida dengan saiz busa antara $70\mu\text{m}$ hingga $150\mu\text{m}$, keliangan 77% hingga 90% sebagai kriteria pemangkin di dalam pembaharuan wap methana (SMR). Kajian ini, busa SiO_2 dan busa $\text{SiO}_2\text{-NiO}$ dihasilkan menggunakan teknik busa replikasi. Dalam kajian ini, busa SiO_2 dan busa $\text{SiO}_2\text{-NiO}$ dihasilkan menggunakan teknik replikasi busa. Sampel yang dihasilkan juga menggunakan komposisi serbuk SiO_2 yang berbeza hasil daripada abu sekam padi (RHA) (20% hingga 35%) dan suhu sinter antara 850°C hingga 1250°C . Pencirian terhadap busa SiO_2 dan $\text{SiO}_2\text{-NiO}$ telah dilakukan antaranya adalah ujian morfologi, keliangan, ketumpatan dan kekuatan busa bagi memenuhi kriteria sebagai pemangkin di dalam SMR. Morfologi menunjukkan saiz liang yang terbuka antara $15.13\mu\text{m}$ sehingga $76.06\mu\text{m}$ dengan sangga bersambung dan liang yang rapat. Keputusan keliangan menunjukkan nilai paling rendah ialah 65% dan tertinggi adalah 81.74% manakala nilai ketumpatan terendah dan tertinggi masing-masing adalah 0.626 g/cm^3 dan 1.070 g/cm^3 . Justeru itu, keputusan bagi kekuatan mampatan adalah dalam julat 0.06 MPa hingga 0.47MPa. Hasilnya, busa $\text{SiO}_2\text{-NiO}$ (35 wt% SiO_2 dengan 5 wt% NiO) yang dihasilkan didapati mempunyai sifat mekanik dan fizikal yang lebih sesuai untuk pemangkin penapis dalam pembentukan metana wap (SMR). Keputusan penukaran metana (CH_4) menunjukkan busa $\text{SiO}_2\text{-NiO}$ menghasilkan antara julat 34.72% hingga 42.6% dan hasilnya membuktikan bahawa busa silika daripada abu sekam padi dan NiO amat sesuai digunakan sebagai pemangkin di dalam aplikasi SMR dimana pencapaian CH_4 melebihi daripada 21%

LIST OF CONTENTS

TITLE	i
DECLARATION	ii
ACKNOWLEDGEMENT	iv
ABSTRACT	v
ABSTRAK	vi
LIST OF CONTENTS	vii
LIST OF TABLES	xi
LIST OF FIGURES	xiii
LIST OF SYMBOLS AND ABBREVIATIONS	xviii
CHAPTER 1 INTRODUCTION	1
1.1 Background of the study	1
1.2 Problem Statement	4
1.3 Objectives	6
1.4 Scope of Study	6
1.5 Novelty and Contribution	7
CHAPTER 2 LITERATURE REVIEW	9
2.1 Introduction to Catalytic Reforming Technologies	9
2.2 Steam Methane Reforming (SMR)	11
2.3 Catalyst support	14
2.4 Characteristics and Properties of Porous Ceramic for Catalytic Performance	15
2.5 Porous Ceramic As Catalyst	16

2.6	Fabrication of Porous Material	21
2.6.1	Foam replication method	21
2.7	Sintering Process	29
2.8	Effects of Composition on Fabrication of Foam	35
2.9	Silica (SiO_2) and Nickel Oxide (NiO) Compatibility	38
2.9.1	Silica (SiO_2)	38
2.9.1.1	Silica (SiO_2) derived from Rice Husk Ash (RHA)	39
2.9.2	Nickel oxide (NiO)	42
2.10	Polyvinyl Alcohol (PVA) as a Binder	43
2.11	Function of Silica Foam As Methane Reforming Catalyst	45
2.11.1	Physical characterisations and properties	46
2.11.1.1	Silica (SiO_2) derived from rice husk as (RHA)	46
2.11.2	Morphology of SiO_2 foam by FESEM	48
2.12	Additive Nickel Oxide (NiO) for the Reforming of Methane	51
2.12.1	Function of NiO as a catalyst	51
2.12.2	Physical characterisations of NiO	51
2.12.2.1	Characterisation NiO by X-Ray Diffraction (XRD)	52
2.13	Silica and Nickel Foam As Catalysts in Methane Reforming	55
2.13.1	Effect of temperature on methane conversion	56
CHAPTER 3 METHODOLOGY		60
3.1	Introduction	60
3.2	First Stage: Derivation of SiO_2 from RHA, Raw Materials and Equipment	62



3.3	Characterisation of Raw Material	64
3.4	Preliminary Study	65
3.5	Fabrication of Porous Body	65
3.6	Raw Material and Equipment	71
3.7	Designation of Sample	72
3.8	Analyses method	72
3.8.1	Raw materials, SiO ₂ foam and SiO ₂ -NiO foam	72
3.8.1.1	Elemental analysis	74
3.8.1.2	Phase analysis	74
3.8.1.3	Morphology analyses	75
3.8.1.4	Thermal properties analysis	76
3.8.1.5	Shrinkage	77
3.8.1.6	Porosity and density	78
3.8.1.7	Compressive test	78
3.9	Steam Methane Reforming Method	79
3.10	Gas Chromatography (GC) Test	82
CHAPTER 4 RESULT AND DISCUSSION		84
4.1	Characterization of SiO ₂ as derived from RHA	84
4.1.1	Phase Analyses	84
4.1.2	Morphological Analyses	86
4.1.3	Elemental composition Analyses	87
4.1.4	Thermal analyses of Silica (SiO ₂) as derived from RHA	90
4.2	Characterization of PVA and PU sponge.	90
4.2.1	Thermal analyses of PVA	90
4.2.2	Thermal analyses of Polyurethane foam (PU)	91
4.2.3	Morphology analyses of PU foam	93
4.3	Characterization of NiO	93
4.3.1	Phase analyses	93
4.3.2	Morphological analyses	94



4.4	Preliminary work for parameter determination in SiO ₂ -NiO fabrication	95
4.4.1	Selection of SiO ₂ -NiO slurry composition	95
4.4.2	Compatibility between SiO ₂ as derived from RHA and NiO	99
4.5	Effect of SiO ₂ (as derived from RHA) compositions and NiO addition on fabricated of SiO ₂ foam and SiO ₂ -NiO foam	101
4.5.1	Visual observation of foam	101
4.5.2	Morphology of foam	102
4.5.3	Shrinkage of foam	104
4.5.4	Apparent Porosity and density analyses	107
4.5.5	Compressive strength of the foam	112
4.6	Effect of sintering temperature in the fabrication of porous body	114
4.6.1	Colour observation	114
4.6.2	Morphology analyses	116
4.6.3	Shrinkage analysis	118
4.6.4	Apparent Porosity and density analysis	121
4.6.5	Compressive strength analyses	126
4.7	Catalytic Behavior of SiO ₂ -NiO foam on Steam Methane Reforming (SMR) Yields	129
4.7.1	Activation of NiO supported SiO ₂ foam as a catalyst	129
CHAPTER 5 CONCLUSION AND RECOMMENDATION		133
5.1	Conclusion	133
5.2	Recommendation	134
REFERENCES		136

LIST OF TABLES

2.1	Structure of ceramic foam	18
2.2	Type of pores in ceramic foam	19
2.3	Examples of replica method reported in the literature	25
2.4	Microstructure and properties of porous materials prepared by the foam replication method	27
2.5	Properties of ceramic foam	29
2.6	Effects of sintering temperature on ceramic foam	31
2.7	Typical properties of SiO ₂	39
2.8	Comparison of the different chemical compounds obtained from different types of silica	41
2.9	Properties of nickel oxide (NiO)	42
2.10	Advantages of PVA	44
2.11	Typical properties of PVA (Mittal, 2010), PEG and CMC	44
2.12	Comparison of XRD pattern by different researchers	47
2.13	Comparison of XRD patterns of NiO	53
3.1	Compositions of SiO ₂ , NiO, PVA and distilled water	66
3.2	Details of raw materials	71
3.3	Details of equipment	71
3.4	Tests and standards used in the study	73
3.5	JCPDS file numbers for SiO ₂ and NiO	74
4.1	Position of the amorphous halo of SiO ₂ as derived from RHA (present study and literature)	85
4.2	Elemental existed in SiO ₂ as derived from RHA	87
4.3	Compares the element composition SiO ₂ as derived from RHA	89

4.4	Summary of slurry condition (viscosity and absorption capability)	97
4.5	Observation on the workable slurry of SiO_2 -NiO for the foam fabrication	98
4.6	CH_4 conversion of SiO_2 –NiO catalyst	132



PTTA UTHM
PERPUSTAKAAN TUNKU TUN AMINAH

LIST OF FIGURES

2.1	Types of catalytic reforming	10
2.2	Group 8–10 of noble metals	12
2.3	Types of porous ceramic	17
2.4	Three-dimensional images of ceramic foams:	
	a) open pores and b) closed pores	18
2.5	Examples of cells of ceramic foam:	
	a) pore, window and strut, b) closed pores and c) open pores	19
2.6	Schematic of classification of porous ceramics	20
2.7	Schematic drawing of direct foaming method for fabrication of ceramic foam	23
2.8	Process preparation of ceramic foam by using the polymeric sponge method	23
2.19	Average pore size from the replica method	28
2.10	Density and compressive strength of ceramic foam via the replica method	28
2.11	Sintering profile	30
2.12	Stages of sintering process: initial stage (left), intermediate stage (centre) and final stage (right)	30
2.13	Effect of sintering temperature on ceramic filter	32
2.14	Effect on the density of the specimen sintered at different temperatures	33
2.15	Effect of sintering temperature on shrinkage	34
2.16	Effect of sintering temperature on density	35
2.17	Porosity with different composition SiO_2	36
2.18	Bulk density with different composition SiO_2	36

2.19	Compressive strength vs. increasing content CaO	37
2.20	Chemical structure of silica	38
2.21	Overview of silica from rice husk ash (RHA)	40
2.22	Phases of silica derived from rice husks	41
2.23	Chemical structure of nickel oxide (NiO)	42
2.24	The chemical structure of polyvinyl alcohol (PVA)	44
2.25	XRD pattern for amorphous silica	46
2.26	XRD pattern for silica produced from rice husks)	47
2.27	FESEM micrographs at low magnification (a and d), medium magnification (b and e) and high magnification (c and f) for SiO ₂ /PAM composite	48
2.28	FESEM morphology for amorphous silica at different magnifications	49
2.29	SEM images of controlled pore size of porous silica foam	50
2.30	Morphology of porous silica ceramic	50
2.31	XRD spectra of nickel oxide	52
2.32	SEM micrographs of pure Ni foam surface taken at 100× magnification	53
2.33	Morphology of silica-nickel oxide foam	54
2.34	Macromorphology of nickel foam	55
2.35	Effect of temperature on CH ₄ conversion	56
2.36	Effect of temperature on CH ₄ conversion	57
2.37	Effect of temperature on the conversion of methane	57
2.38	CH ₄ conversion at different reaction temperatures	58
3.1	The overall stages of research methodology	61
3.2	1 st stage of experiment procedure: Derivation of silica (SiO ₂) from rice husk ash (RHA)	62
3.3	Rice husks conversion to silica powder	64
3.4	Firing profile for preparation of RHA	65
3.5	2 nd stage of experiment procedure: Characterisations of raw materials	64
3.6	3 rd stage of experiment procedure: Preliminary compability of SiO ₂ and NiO	65



3.7	4 th stage of experiment procedure: Fabrication of porous body	63
3.8	Cutting off the PU sponge	63
3.9	PU foam after being cut off	69
3.10	Mixing process to fabricate a slurry	69
3.11	Consolidation of PU foam into a slurry	70
3.12	Sintering profile for SiO ₂ and SiO ₂ -NiO foams	70
3.13	Designation of samples for SiO ₂ and SiO ₂ -NiO foam	72
3.14	Samples for SEM: a) PU foam and b) SiO ₂ -NiO foam	75
3.15	Top view of sample position	76
3.16	Schematic of the study's TGA	77
3.17	a) Universal testing machine (EHF-EM0100K1, Servopulser, Shimadzu, Japan) and b) fracture on the foam	79
3.18	5 th stage of experiment procedure: Steam methane reforming conversion	80
3.19	Tedlar sampling bag	80
3.20	Box furnace Steam methane reforming (SMR) rig	81
3.21	Packed bed reactor	81
3.22	Schematic drawing of the experiment setup	82
3.23	Schematic diagram of gas chromatography	83
4.1	XRD pattern for SiO ₂ powder as derived from RHA	84
4.2	Microstructure of SiO ₂ powder as derived from RHA (350 magnification)	86
4.3	a) Rice husk ash b) Powder Silica as derived from RHA	88
4.4	TGA of SiO ₂ as derived from RHA	90
4.5	TGA of PVA	91
4.6	Thermal gravimetric analysis for PU foam	92
4.7	Morphology of PU foam (150 magnification)	93
4.8	XRD pattern of NiO	94
4.9	FESEM micrograph of NiO powder (10 000 magnification)	95
4.10	Condition (a) low (b) moderate (c) high slurry	96
4.11	Compatibility of SiO ₂ as derived from RHA and NiO of different composition at 850°C	99

4.12	Phase change mechanism: the phase material changes from (a) amorphous phase (b) crystalline	100
4.13	Visual observation of PU foam a) original PU foam b) after impregnation slurry onto PU foam	101
4.14	Visual observation of porous body a) SiO ₂ foam b) SiO ₂ -NiO foam	102
4.15	Microstructure of SiO ₂ foam at a) 20wt. % b) 25wt % c) 30wt% d) 35wt% composition of SiO ₂	102
4.16	Microstructure of SiO ₂ -NiO foam at the different composition of SiO ₂ RHA a) 20wt% b) 25wt% c) 30wt% d) 35wt%	103
4.17	Shrinkage of SiO ₂ foam	104
4.18	Mechanism of the shrinkage.	105
4.19	Shrinkage of SiO ₂ -NiO foam at the different of SiO ₂ as derived from RHA composition with 5wt% NiO addition	106
4.20	Mechanism shrinkage of SiO ₂ -NiO foam	107
4.21	Apparent porosity of SiO ₂ foam at different SiO ₂ as derived from RHA	108
4.22	Apparent porosity of SiO ₂ -NiO foam at different SiO ₂ as derived from RHA composition with 5wt% NiO addition	108
4.23	Bulk density of SiO ₂ foam at different SiO ₂ as derived from RHA composition	110
4.24	Bulk density of SiO ₂ -NiO foam at different SiO ₂ as derived from RHA with 5wt% NiO addition	111
4.25	Compressive strength of SiO ₂ foam at different SiO ₂ as derived from RHA composition	112
4.26	Compressive strength of SiO ₂ -NiO foam at different SiO ₂ as derived from RHA composition with 5wt% NiO addition	113
4.27	Visual observation of SiO ₂ foam and SiO ₂ -NiO foam before and after sintering (850, 950, 1050, 1150 and 1250°C)	115



4.28	Microstructure of SiO ₂ foam sintered from 850°C to 1250°C	116
4.29	Morphology of SiO ₂ -NiO foam at different sintering temperature from 850°C to 1250°C	117
4.30	Shrinkage of SiO ₂ foam at different sintering temperatures	119
4.31	Shrinkage of SiO ₂ -NiO foam at different sintering temperature.	120
4.32	Mechanism of shrinkage, the effect of sintering temperatures on SiO ₂ -NiO foam	121
4.33	Percentage of porosity SiO ₂ foam at different sintering temperature	122
4.34	Apparent porosity of SiO ₂ -NiO foam at different sintering temperatures.	123
4.35	Bulk density of SiO ₂ foam at different sintering temperatures.	125
4.36	Bulk density of SiO ₂ -NiO foam at different temperatures	126
4.37	Compressive strength of SiO ₂ foam at different sintering temperatures.	127
4.38	Compressive strength of SiO ₂ -NiO foam at different sintering temperatures	128
4.39	TPR profile SiO ₂ -NiO catalyst	129
4.40	CH ₄ conversion by NiO supported SiO ₂ catalyst	131



LIST OF SYMBOLS AND ABBREVIATIONS

SiO ₂	- Silica/ silicon dioxide
RHA	- Rice Husk Ash
Kg	- kilogram
kg/m ³	- kilogram per cubic metre
K ₂ O	- Potassium oxide
Al ₂ O ₃	- Aluminium oxide
CaO	- Calcium oxide
MgO	- Magnesium oxide
Na ₂ O	- Sodium oxide
Fe ₂ O ₃	- Iron (III) oxide
g/cm ³	- gram per cubic centimetre
Ni	- Nickel
SMR	- Steam Methane Reforming
hr	- hour
mm	- millimetre
NiO	- Nickel Oxide
PVA	- Polyvinyl alcohol
SEM	- Scanning electron microscope
XRD	- X-Ray Diffraction
GC	- Gas Chromatography
POX	- Partial oxidation
CH ₄	- Methane
H ₂	- Hydrogen
CO	- Carbon monoxide
MgO	- Magnesium Oxide
nm	- Nanometer

NiO/ZnO.	- Nickel oxide/Zinc oxide
μm	- micrometer
PU	- Polyurethane
TGA	- Thermal gravity analysis
MPa	- Megapascal
$^{\circ}\text{C}/\text{min}$	- Celsius per minute
kN	- Kilonewton
ASTM	- <i>American Society for Testing and Materials</i>
Si_3N_4	- Silicon nitride
SS 316L	- 316L stainless steel
Al	- Aluminum
Mg	- Magnesium
Ni_2SiO_4	- Nickel silicate
2θ	-2 theta
FESEM	- Field Emission Scanning Electron Microscope
JCPDS	- The Joint Committee on Powder Diffraction Standards
rpm	- revolution per minute
g	- gram
XRF	- X-Ray Fluorescence
ml	- Milliliter
TPR	- Temperature Programmed Reduction



CHAPTER 1

INTRODUCTION

1.1 Background of the study

The Green Technology Master Plan (GTMP) is an outcome of the Eleventh Malaysia Plan (2016–2020), which has earmarked green growth as one of six game-changers to alter the trajectory of the nation's growth. The National Green Technology Policy is built on four pillars, which are Energy, Environment, Economy and Social. Green technology is aimed to be the key driver in accelerating the national economy and promoting sustainable development in Malaysia (Ministry of Energy, Green Technology and Water, 2017). There have been numerous innovations of technology being utilised in daily life. Examples of technologies that are widely used are cars, buses and motorcycles in the field transportation and electrical insulators and tiles in buildings and the aerospace industry, as well as innovations in the medical field. Among the most significant innovations are the materials used to build these products, such as metals, ceramics, plastics, polymers and many other materials. Different materials have their own properties and specialities to make them better. In this research study, ceramic is the primary material chosen instead of metal for the steam methane reforming applications.

In the fabrication of ceramic foams, a majority of the materials used are costly and not sustainable. In this study, in order to address this issue, the raw materials used were Silica (SiO_2) derived from Rice Husk Ash (RHA) and Nickel Oxide (NiO). Rice husks are among the variety of agricultural wastes or biomasses

available. In addition, silica from rice husk ash is a renewable resource and therefore generates low production costs for the foams (Hossain *et al.*, 2018).

Rice Husk Ash is an agricultural waste material that are produced approximately 100 million tons annually. Approximately 20 kg of rice husks could be produced from 100 kg of rice. RHA has been widely used in the construction industry owing to its high availability, low bulk density (90–150 kg/m³), durability, abrasive character, weather resistance and unique composition (Taufik *et al.*, 2013)

Rice Husk Ash contains 75%–90% organic matters, such as cellulose and lignin, and the rest are mineral components such as silica, alkalis and trace elements. Other constituents of RHA, such as K₂O, Al₂O₃, CaO, MgO, Na₂O, Fe₂O₃, are available at less than 1%. Moreover, RHA has a bulk density of 96–160 kg/m³ and consists of 31%–37% oxygen, 0.2%–0.32% nitrogen and 0.04%–0.08% sulphur (Kumar *et al.*, 2013). The main components in RHA are silica, cellulose and lignin.

Silicon dioxide or silica (SiO₂) is an oxide of the silicon element, which is the second-most abundant element found on earth. Silica has been identified in some way in all natural water resources. In addition, many plants, such as strawberries, avocados, onions, root vegetables, wheat and oats, contain silica and it can also be found in nature as sand, sandstone, quartz, flint, agate or granite (Hossain *et al.*, 2018). Silica has three phases, which are amorphous, crystalline and tridymite. Most silicas exist in the amorphous form, while quartz is the purest form of silica. Other than that, sand and rock are natural sources of silica that are less refined. The three most common polymorphs of crystalline silica are quartz, tridymite and cristobalite (Carcinogen, 2006). Silica-based materials have attracted considerable attention because of their high surface area (>200 m²g⁻¹), ordered pore distribution, narrow pore size, high thermal stability and natural regeneration and reusability in comparison with several soils and soil components. Due to these properties, they are ideal base materials as catalysts, catalyst supports and adsorbents, and as a template for other materials. Silica is attractive as a catalyst support since it has strong structural robustness, is stable even at elevated temperature and is chemically inert (Majewski *et al.*, 2013). Furthermore, a combination of SiO₂ with NiO is a promising solution as a catalyst in the steam methane reforming industry (Bej *et al.*, 2013).

In ceramic applications, silica foams typically show fully open pores, closed pores and partially interconnected porosity. Most applications of porous microspheres centre on the porous structure, such as porosity, pore size and surface

area. Silica foams typically have 70% to 90% porosity, with density varying from 0.4 to 0.7 g/cm³ (Nazaruddin *et al.*, 2017)

Many methods are used in the manufacturing of ceramic foam, such as the replication method, also known as the slurry process, as well as a direct foaming. Among these various types of fabrication method, the slurry method has been chosen to fabricate the ceramic foam-like silica foam. The slurry method was developed by Schwartzwalder and Somer (1963), and presently the ceramic fabrication is by using an open-cell porous product of a synthetic polymer or a natural organic material in a slurry, which is divided into ceramic powder and ceramic binders, to uniformly coat the inner cells forming the walls of an element. The binder composition usually used is about 1% to 5% in order to enhance the compressive strength of the ceramic foam up to 1 to 2 MPa (Han *et al.*, 2002).

For the catalyst process, it is necessary to have high mass, a high heat transfer rate and a wide contact surface in order to achieve excellent catalytic reaction performance. Nickel (Ni) has emerged as a new metal with catalytic power towards oxygen evolution, and great efforts have been put to develop Ni-based catalysts, including oxides, hydroxides, sulphides and nitrides in alkaline solution (Liang *et al.*, 2015). A Ni-based catalyst is often considered as a catalyst for steam reforming due to its high tar destruction activity. It is evident that the selection of the support material is considered as one of the particularly crucial issues in tar steam reforming for hydrogen production. The most commonly used supports are minerals and alumina or modified alumina (Gao *et al.*, 2015) which the high cost of material.

Nickel is considered to be one of the best non-noble catalyst materials for hydrogen evolution reaction (HER). This is mainly due to the fact that Ni is primarily resistant to corrosion at high pH values and also due to the particular importance of nickel's structure having a large specific surface area (large roughness) (Pierozynski *et al.*, 2014). Ni has comparable activities to noble-metal catalysts, and that a higher loading amount of Ni is feasible in terms of catalyst cost in order to increase the activity per catalyst volume. Although Ni is inferior to noble metals in regards to the resistance to carbon deposition and catalyst oxidation, the high resistance to coke formation and catalyst oxidation can be realised by the addition of minimal amounts of noble metals (Wu *et al.*, 2013).

In this study, nickel oxide was preferred as the silica foam support because of the lower price as it is derived from the RHA foam. This would lead to the high

ability of the silica itself in the absorption of substances and to obtaining good strength and hardness properties in the ceramic products because firing rice husks at high temperature generates high strength (Zainal *et al.*, 2019). As the field of technical ceramics continues to expand, the use of ceramic materials as catalyst support is opening several opportunities for the review of applications, preparation and stability of porous ceramic materials. Ceramic foams have been used as catalyst supports in the areas of ammonia oxidation, catalytic combustion, partial oxidation, steam reforming and exhaust catalysis. More works have since appeared on foam-supported catalysts for methane or propane combustions. Steam reforming of methane from biogas at a small scale could potentially provide a source of hydrogen for applications such as electricity generation via fuel cells. The efficiency of the reforming process is dependent upon an active catalyst, and thus this present work aimed to produce a highly active catalyst for methane reforming that is resistant to deactivation (Majewski *et al.*, 2013).

Furthermore, steam methane reforming (SMR) can be catalysed by several metal catalysts. For instance, cobalt, platinum, palladium, iridium, ruthenium, rhodium and nickel have all been cited as usable for this purpose. Even in the light of this, as one of the relatively lower-activity metals, nickel has become the industry-standard catalytic metal used in steam methane reforming because of its relatively low cost, wide availability and sufficient catalytic activity, all combining to make it the most cost-efficient choice (Meloni *et al.*, 2020).

This study focuses on the compatibility of RHA-derived silica with the addition of nickel oxide for the fabrication of ceramic foams as the steam methane reforming catalyst.

1.2 Problem Statement

Rice husks (RH) are bulky agricultural wastes with an annual world production of approximately 100 million tons. Most of the husks produced from rice processing are currently either burned or dumped as waste thus causing damage to the land and environmental pollution (Azmi *et al.*, 2016). Besides that, it has been reported that at 600 to 1000°C, amorphous silica is formed. Therefore, to solve energy problem, the burning temperature at 450°C was used in producing of silica as a catalyst.

Furthermore, in catalyst, most of researchers used a metal as a catalyst carrier. Mostly a metal are limited high cost and rusty when reaction with the steam (Wang *et.al.*, 2020). The improvement, this study are used the ceramic material (SiO_2) due to low cost and rust resistant.

In previous studies, there are several factors, such as the type of raw material, material composition, size of the raw material, fabrication method, type of binder and binder distribution, that affect the morphological, physical and mechanical properties of porous ceramic foams (Baharom, 2014). However, choosing the appropriate manufacturing process is very important since the pore distribution, size, shape and volume porosity of the porous material produced depends on the type of fabrication method used. It is known that, the pore structure of the cancellous bone is open and interconnected. Therefore, fabrication methods that can produce such open and interconnected pore structure need to be identified. Some of researchers used the compaction method to fabricate ceramic foams. This method consists of five major steps: powder selection, mixing, compacting, sintering and spacer removal (Ahmad & Kassim, 2011). However, this method has some problems, such as the pressing speed and the releasing speed of the punch usually leading to the crack formation of the compacted parts. Too high of a punch speed will result in a higher density at the contacting surface, which is susceptible to cracks. Meanwhile, too high of a releasing speed will discharge the internal pressure too quickly and lead to cracks (Baharom, 2014). Foam replication is a very economical powder metallurgical method for producing porous materials with open and interconnected pores, and also with a unique combination of properties that is suitable for various applications. It is possible to fully transform the open and interconnected pores of PU foam into open and interconnected pores of the porous ceramic. To date, there has been limited comprehensive research that studies the parameters involved in each processing step for the fabrication of porous SiO_2 and NiO with open and interconnected pores using foam replication methods especially for applications as catalyst in SMR.

In addition, one of the challenges in selecting the appropriate temperature for foam manufacturing is to avoid fabricating porous ceramics with low strength. Hence, the current study can be reduced using adequate heating and regulation of the environment, such as a low heating and cooling rate of $2^\circ\text{C}/\text{min}$, which would result in a sintered body that does not crack. Beside that, the temperature used in fabrication of ceramic foam required the high temperature as 1450°C and its should

be more energy to handle it. So, to reduce of the high energy the low temperature below to 1250°C were choose in this research.

The catalytic process affects the chemical reaction and production of the synthesis gas (hydrogen). Common noble-metal catalysts used include ruthenium, rhodium and platinum. Noble metal sources are limited, expensive and resistant to chemical reactions (Wang *et al.*, 2020). A solution to the noble metal problem is using another type of catalyst, which is the nickel-based catalyst. This low-cost catalyst has a high propensity to carbon deposition through the steam methane reforming (SMR) cycle (Zhang *et al.*, 2015).

1.3 Objectives

The objectives of this study are as follows:

- 1) To elucidate the suitable composition of SiO₂ and NiO for the SiO₂-NiO foam fabrication.
- 2) To examine the physical and mechanical properties of the SiO₂ and SiO₂-NiO foams fabricated with different compositions and at different sintering temperatures.
- 3) To examine the capability of the SiO₂ and SiO₂-NiO foams as a catalyst in the steam methane reforming process.

1.4 Scope of Study

The scope of the study was designed so that the objectives are met and to avoid deviating the results of the study from the desired objectives. The scope of study is as follows:

- 1) Producing of SiO₂ as derived from Rice Husk Ash (RHA) at temperature 450°C for 8 hrs with a heating rate of 10°C/min.
- 2) Composition of the SiO₂-NiO foam:
 - a) SiO₂ compositions used were 20 wt%, 25 wt%, 30 wt%, 35 wt%, 40 wt%, 45 wt%, 50 wt% and 55 wt%.
 - b) Nickel oxide's compositions: 0 wt%, 5 wt%, 10 wt%, 15 wt%, 20 wt% and 25 wt%.

- c) PVA was used as a binder at 5 wt%
- 3) Phase compatibility studies were conducted on the SiO₂-NiO foam at sintering temperatures of 850°C, 950°C, 1050°C, 1150°C and 1250°C.
- 4) The characterisations of the raw materials include:
 - a) Morphology analysis – Scanning Electron Microscopy (SEM)
 - b) Phase analysis – X-Ray Diffraction (XRD)
 - c) Elemental analysis – X-Ray Fluorescence (XRF)
 - d) Thermal analysis – Thermogravimetric analysis (TGA)
- 5) The characterisation tests of the SiO₂-NiO ceramic foam include:
 - a) Morphology analysis – Scanning Electron Microscopy (SEM)
 - b) Phase analysis – X-Ray Diffraction (XRD)
 - c) Physical properties such as density, porosity and shrinkage were examined.
 - d) A compressive test was conducted to identify the strength properties of the SiO₂-NiO foam.
- 6) Steam methane reforming test of the SiO₂-NiO foam was conducted using Gas Chromatography (GC) to identify the catalytic capability of the SiO₂-NiO foam. The sample used for the catalytic process in SMR was 35wt% SiO₂ with 5wt% NiO and the catalyst reaction temperature are 500, 550 and 600°C.

1.5 Novelty and Contribution

This section describes the significant findings and the novelty contributed by this study.

The derivation of SiO₂ from RHA was conducted by burning the rice husks at 450°C. Based on the review of the latest literature, the derivation of SiO₂ are burning at 600°C and most silicas used in the fabrication of ceramic foams are commercial silica. Thus far, the literature on the study regarding SiO₂ from RHA in the fabrication of ceramic foams is limited.

In addition, the combination of RHA-derived SiO₂ and NiO in the fabrication of ceramic foams is yet to be investigated and reported, as confirmed by the literature review to date. Moreover, the properties of a foam using RHA-derived SiO₂ and NiO

fabricated via the replica method has never been investigated, as evidenced by the review of previous studies.

In terms of catalyst application, there have been no studies reported in the literature on the analysis of methane conversion using the combination of RHA-derived SiO_2 and NiO and the reaction temperature in SMR at low temperature (500-600°C).



PTTA UTHM
PERPUSTAKAAN TUNKU TUN AMINAH

CHAPTER 2

LITERATURE REVIEW

2.1 Introduction to Catalytic Reforming Technologies

Recently, hydrogen has become a promising energy carrier since it has high energy density and generates no pollutants during its combustion, which reduces the impact on the environment significantly. Future applications of hydrogen as an energy carrier will provide effective, clean and recyclable energy, and its combustion releases a remarkable amount of energy per unit weight. Hydrogen can be used in a variety of applications, for example, as fuel for fuel cells and internal combustion engines and as a reactant in the hydrogenation process. In industrial production, the preparation of hydrogen is widely studied, and it is usually produced via steam reforming of traditional fossil resources. Currently, due to the abundant natural gas reserves, methane is widely used in hydrogen production. Among the different production methods of hydrogen, the steam reforming of methane is one of the most widely used (Wang *et al.*, 2020). A hydrogen economy has become an interest in the world (Belhadi *et al.*, 2016). Steam reforming reactions will play a key role in new applications of synthesis gas and in the future hydrogen economy.

As explained by Madon *et al.* (2018), the world's energy sources are being threatened by the increasing demand for energy consumption. Hydrogen as a potential alternative energy source and energy carrier has been explored to address such needs. This is because hydrogen is widely accepted as the cleanest, efficient and pollution-free energy source. The production of hydrogen from various hydrocarbons, especially methane, mainly comes from the chemical reaction processes of the

catalytic reforming technologies, such as steam reforming, partial oxidation and autothermal reforming. Among these, steam methane reforming (SMR) has the advantages of relatively low reaction temperature and high hydrogen content in the reforming products (Madon *et al.*, 2016; Wang *et al.*, 2013; Matsumura *et al.*, 2004). Types of catalytic reforming are graphically illustrated in Figure 2.1.

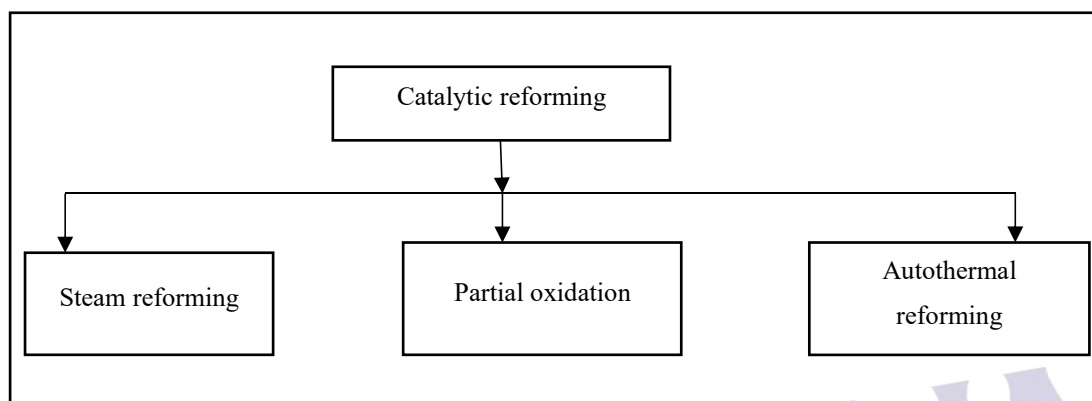


Figure 2.1 :Type of catalytic reforming (Madon *et al.*, 2018)

Steam reforming uses an external source of hot gas to heat tubes in which the catalytic reaction takes place, which converts steam and lighter hydrocarbons such as methane, biogas or refinery feedstock into hydrogen (H_2) and carbon monoxide (CO) (syngas). Syngas reacts further to give more hydrogen and carbon dioxide in the reactor.

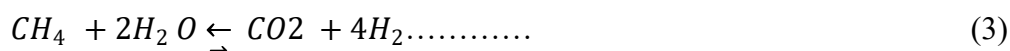
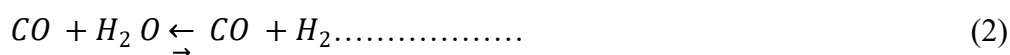
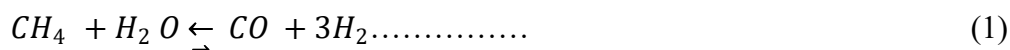
Meanwhile, autothermal reforming is grouped under partial oxidation, which uses oxygen and carbon dioxide or steam in a reaction with methane to form synthesis gas. The reaction takes place in a single chamber where the methane is partially oxidised. The reaction is exothermic due to the oxidation. The main difference between autothermal reforming and steam methane reforming is that steam methane reforming does not use or require oxygen. The advantage of autothermal reforming is that H_2/CO can be varied, which is particularly useful for producing certain second-generation biofuels such as dimethyl ether synthesis (Speight, 2015). However, it is less efficient in producing hydrogen (Liu, 2006).

Partial oxidation (POX), on the other hand, is a type of chemical reaction. It occurs when a quantity of reactants of fuel-air mixture is partially combusted in a reformer, creating a hydrogen-rich syngas, which can then be put to further use. The

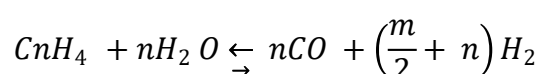
oxidation causes the reaction to be exothermic (a chemical reaction that releases energy through light or heat). Catalytic partial oxidation does not involve operating at very elevated temperatures but involves the removal of sulphur, which poisons the catalyst. High-temperature partial oxidation can also manage much heavier oil fractions than the catalytic process and is therefore appealing for the processing of diesel, logistic fuels and remaining fractions. These fuels are removed in large-scale activities, but it is hard to scale and regulate the process. Nickel is one of the most widely used active phases in partial oxidation (Galvan *et al.*, 2019). Partial oxidation, however, generates less hydrogen per methane molecule. This implies that partial oxidation is less effective than steam reforming for fuel cell applications.

2.2 Steam Methane Reforming (SMR)

Traditional steam methane reforming plants for hydrogen production not only consume large amounts of natural gas but also emit a lot of greenhouse gases (Li *et al.*, 2020). Due to its clean and renewable nature, hydrogen has attracted considerable attention. The technical routes for hydrogen production to date include mainly water electrolysis and steam methane reforming (SMR). SMR has been the preferred technology for the industrial production of synthesis gas from methane to produce ammonia or methanol. This is an important technology pathway for the production of near-term hydrogen. Steam reforming of methane consists of three reversible reactions: the strongly endothermic reforming reactions 1 and 3, and the moderately exothermic water-gas shift (WGS) reaction 2 (Galvan *et al.*, 2019).



The basic reforming reaction for a generic hydrocarbon methane (C_nH_m) is as follows:



Proton Number

Relative Atomic Mass

Symbol

Element Name

GROUP 8-10 noble metals

Metal

Semi-Metal

Non-metal

1 2

3 4 5 6 7 8 9 10 11 12

13 14 15 16 17 18

19 20 21 22 23 24 25 26 27 28 29 30 31 32 33 34 35 36 37 38 39 40 41 42 43 44 45 46 47 48 49 50 51 52 53 54 55 56 57 58 59 60 61 62 63 64 65 66 67 68 69 70 71 72 73 74 75 76 77 78 79 80 81 82 83 84 85 86 87 88 89 90 91 92 93 94 95 96 97 98 99 100 101 102 103 104 105 106 107 108 109 110 111 112 113 114 115 116 117 118 119 120 121 122 123 124 125 126 127 128 129 130 131 132 133 134 135 136 137 138 139 140 141 142 143 144 145 146 147 148 149 150 151 152 153 154 155 156 157 158 159 160 161 162 163 164 165 166 167 168 169 170 171 172 173 174 175 176 177 178 179 180 181 182 183 184 185 186 187 188 189 190 191 192 193 194 195 196 197 198 199 200 201 202 203 204 205 206 207 208 209 210 211 212 213 214 215 216 217 218 219 220 221 222 223 224 225 226 227 228 229 230 231 232 233 234 235 236 237 238 239 240 241 242 243 244 245 246 247 248 249 250 251 252 253 254 255 256 257 258 259 260 261 262 263 264 265 266 267 268 269 270 271 272 273 274 275 276 277 278 279 280 281 282 283 284 285 286 287 288 289 290 291 292 293 294 295 296 297 298 299 300 301 302 303 304 305 306 307 308 309 310 311 312 313 314 315 316 317 318 319 320 321 322 323 324 325 326 327 328 329 330 331 332 333 334 335 336 337 338 339 340 341 342 343 344 345 346 347 348 349 350 351 352 353 354 355 356 357 358 359 360 361 362 363 364 365 366 367 368 369 370 371 372 373 374 375 376 377 378 379 380 381 382 383 384 385 386 387 388 389 390 391 392 393 394 395 396 397 398 399 400 401 402 403 404 405 406 407 408 409 410 411 412 413 414 415 416 417 418 419 420 421 422 423 424 425 426 427 428 429 430 431 432 433 434 435 436 437 438 439 440 441 442 443 444 445 446 447 448 449 450 451 452 453 454 455 456 457 458 459 460 461 462 463 464 465 466 467 468 469 470 471 472 473 474 475 476 477 478 479 480 481 482 483 484 485 486 487 488 489 490 491 492 493 494 495 496 497 498 499 500 501 502 503 504 505 506 507 508 509 510 511 512 513 514 515 516 517 518 519 520 521 522 523 524 525 526 527 528 529 530 531 532 533 534 535 536 537 538 539 540 541 542 543 544 545 546 547 548 549 550 551 552 553 554 555 556 557 558 559 560 561 562 563 564 565 566 567 568 569 570 571 572 573 574 575 576 577 578 579 580 581 582 583 584 585 586 587 588 589 590 591 592 593 594 595 596 597 598 599 600 601 602 603 604 605 606 607 608 609 610 611 612 613 614 615 616 617 618 619 620 621 622 623 624 625 626 627 628 629 630 631 632 633 634 635 636 637 638 639 640 641 642 643 644 645 646 647 648 649 650 651 652 653 654 655 656 657 658 659 660 661 662 663 664 665 666 667 668 669 670 671 672 673 674 675 676 677 678 679 680 681 682 683 684 685 686 687 688 689 690 691 692 693 694 695 696 697 698 699 700 701 702 703 704 705 706 707 708 709 710 711 712 713 714 715 716 717 718 719 720 721 722 723 724 725 726 727 728 729 730 731 732 733 734 735 736 737 738 739 740 741 742 743 744 745 746 747 748 749 750 751 752 753 754 755 756 757 758 759 760 761 762 763 764 765 766 767 768 769 770 771 772 773 774 775 776 777 778 779 780 781 782 783 784 785 786 787 788 789 790 791 792 793 794 795 796 797 798 799 800 801 802 803 804 805 806 807 808 809 810 811 812 813 814 815 816 817 818 819 820 821 822 823 824 825 826 827 828 829 830 831 832 833 834 835 836 837 838 839 840 841 842 843 844 845 846 847 848 849 850 851 852 853 854 855 856 857 858 859 860 861 862 863 864 865 866 867 868 869 870 871 872 873 874 875 876 877 878 879 880 881 882 883 884 885 886 887 888 889 890 891 892 893 894 895 896 897 898 899 900 901 902 903 904 905 906 907 908 909 910 911 912 913 914 915 916 917 918 919 920 921 922 923 924 925 926 927 928 929 930 931 932 933 934 935 936 937 938 939 940 941 942 943 944 945 946 947 948 949 950 951 952 953 954 955 956 957 958 959 960 961 962 963 964 965 966 967 968 969 970 971 9

Steam reforming is the most significant path for the large-scale production of ammonia, methanol and other petrochemical synthesis gas and for the production of hydrogen for refineries. In particular, the reforming responses are catalysed by Group 8–10 noble metals (Figure 2.2). However, iron is easily oxidized, cobalt is unable to withstand the partial steam pressure and precious metals (rhodium, ruthenium, platinum and palladium) are too expensive for industrial use (Meloni *et al.*, 2020).

Ni-based catalysts have been intensively studied for methane reforming because of their excellent catalytic performance, wide availability and low cost (Chai *et al.*, 2017; Meloni *et al.*, 2020). Catalytic steam reforming of methane involves the reaction of methane with steam over a catalyst at elevated temperatures (400°C–900°C) and pressures (1–30 atm) (Bej *et al.*, 2013). Ming *et al.* (2002) conducted a 300-h continuous test using a proprietary catalyst for steam reforming of is-octane at 800°C with a steam/carbon ratio of 3:6.

In the past, a great deal of attention has been paid to the preparation of catalysts and the assessment of the process and equipment, with little work being done on the kinetics and mechanism of the reaction. Consequently, there is a lack of kinetic information, and contradictory mechanisms have been suggested. Some early studies, such as by Temkin (1979), have worked on steam methane reforming by investigating the kinetics mainly with Ni catalysts. In the studies, the experiments were performed at temperatures ranging from 470°C–900°C.

The production of synthesis gas from natural gas is one of the important technologies in the chemical industry because synthesis gas can be converted into liquid fuels and chemicals such as methanol and dimethyl ether. Hydrogen is practically produced from natural gas, and the produced hydrogen is mainly used for the ammonia synthesis. In particular, much attention has been paid to the hydrogen production relating to fuel cell technology. The general mechanism for the steam methane reforming is as follows (Beurden, 2004):

- a) Water reacts with surface nickel atoms, yielding adsorbed oxygen and gaseous hydrogen.
- a) The hydrogen formed is directly released into the gas phase, and/or the gaseous H₂ is in equilibrium with the adsorbed H and H₂.
- b) Methane is adsorbed onto the surface nickel atoms. The adsorbed methane either reacts with the adsorbed oxygen or dissociates to form chemisorbed radicals, CH_x with x = 0–3.
- c) The adsorbed oxygen and the carbon-containing radicals react to chemisorb formaldehyde (CH₂O), aldehyde (CHO), CO or CO₂.
- d) CO and CO₂ are formed out of CHO and CH₂O species.

The production of synthetic gas is very significant in the chemical industry for reasons connected to rising oil prices, the depletion of oil reserves and the

environmental issues with exhaust gases. Steam reforming of methane and other hydrocarbons has been an extremely important process to produce synthesis gas. The technology for steam reforming is of great interest because this part of the process represents a substantial portion of the investment costs. The reforming section costs about 60% to 80% of the total cost of the entire gas refining plant. Improvements and cost savings in the reforming section will therefore become very noticeable in the total plant cost (Speight, 2015).

2.3 Catalyst support

The function of the support oxide is not only to control the active metal dispersion but it often also has a significant impact on the catalytic reactions through the metal-supported interactions. A support may play a main role in regulating the size, shape, dispersion and structural stability of metal active locations during the response (Azancot *et al.*, 2019). Noble metals, such as rhodium (Rh), ruthenium (Ru), palladium (Pd) and platinum (Pt), have been reported to offer excellent catalytic performance with higher activity, stability and resistance to carbon deposition for steam methane reforming. However, their high cost limits their use. Therefore, more attention has been focused on the utilisation of cheaper transition metal catalysts, such as nickel (Ni), copper (Cu) and iron (Fe) (Boudjeloud *et al.*, 2019). Ni-based catalysts as low-cost materials are a promising alternative in reforming reactions since they present at high temperatures relatively good activity and high stability (Fang *et al.*, 2016). A typical commercial catalyst uses between 12 wt% to 20 wt% of nickel applied to a refractory ceramic substrate (Dalgleish *et al.*, 2007).

A support determines the dispersion of the catalytically active metal particles and the resistance of the catalyst to sintering. In particular, the function of a support is literally to provide surface assistance for the dispersion of active catalytic metal in order to achieve a stable and highly active metal surface. The most common supports for methane reforming are aluminium oxide (Al_2O_3), magnesium oxide (MgO), magnesium aluminate (MgAl_2O_4), silica (SiO_2), zirconium dioxide (ZrO_2) and titanium dioxide (TiO_2). These supports have a decent porosity, which allows for a more significant surface area. A support plays a crucial role since it determines the final particle size of the metal, its pore structure, its morphology and the phase

transitions that it can undergo. Also, a support can have a chemical role as well, by activating one or more reaction steps.

According to Ozdemir *et al.*, (2010), it was found that Ni/MgO catalyst with 10% Ni content would be the best catalyst and would result in increased CH₄ conversion at temperatures from 500°C to 800°C. Al-Swai *et al.*, (2017) investigated the 10wt% Ni-supported MgO catalyst for the dry reforming of methane reaction at different experiment conditions in a fixed bed reactor with reaction temperatures in the range from 700°C to 900°C, and the catalyst afforded as high as 93% CH₄ conversion at 900°C (Al-Swai *et al.*, 2017)

Bej *et al.*, (2013) reported the alumina-supported nano-NiO catalyst in silica synthesised using the sol-gel method. The NiO crystallite size was found to be 9–15 nm in the Ni loading range of 5%–15%. The catalyst containing 10% Ni was found to be the best for steam reforming reaction in terms of methane conversion. The reaction temperature range was 500°C–700°C and the best reaction condition was established at the temperature of 700°C with 95.7% conversion of methane.

Furthermore, Belhadi *et al.*, (2016) reported the steam reforming of methane performed at 650°C, and the production of hydrogen was observed with the catalyst of 10% NiO/ZnO. The results showed that the catalytic activity in the steam methane reforming was strongly dependent on the percentage of nickel. These results appeared to depend not only on the interaction between nickel and the support but also on the state of the dispersion of nickel on the surface.

2.4 Characteristics and Properties of Porous Ceramic for Catalytic Performance

Porous ceramics, also known as cellular ceramics, was developed in the 1970s. They are made up of a heat-resistant porous material with many gaseous pores. Their pore size ranges mostly between angstrom and millimetre, their porosity normally ranges from 20% to 95% and their production temperature ranges from room temperature to 1600°C. Porous ceramics have several common characteristics (Liu & Chen, 2014):

a) **Good stability**

Choosing the appropriate material species and methods may create porous products suitable for various corrosive circumstances under which the products are supposed to operate.

b) **Great strength and stiffness**

The shape and size of the pores in porous ceramics will not be altered by gas pressure, liquid pressure and other stress loads.

c) **Good thermal stability**

Porous products of heat-resistant ceramics may filter molten steel or high-temperature gas. These outstanding features promise a wonderful future for porous ceramics in a broad range of applications and make these materials adaptable in many fields, including chemical engineering, environmental safety, power sources, metallurgy and the electronics industry.

Generally, porous metals with open-cell structures are necessary for functional applications, since a liquid or a gas medium is required to pass through the porous materials.

According to Twigg *et al.*, (2002), the main characteristics of a ceramic foam for catalyst are sponge-like open structure with pore density of typically 0.02–0.23 g/cm³ creating an interconnecting porosity in the range of 75%–90% or even higher. High porosity ceramics having open pores are considered suitable for catalyst supports because of the low mass-transfer resistance (Yokota *et al.*, 2001).

In addition, Kim *et al.*, (2009) stated that pore size, in particular, is one of the most important properties in determining the practical applications of a ceramic foam when the pore size is approximately 70–150 µm.

2.5 Porous Ceramic As Catalyst

In particular, porous ceramics can be categorised into two primary groups, as illustrated in Figure 2.3.

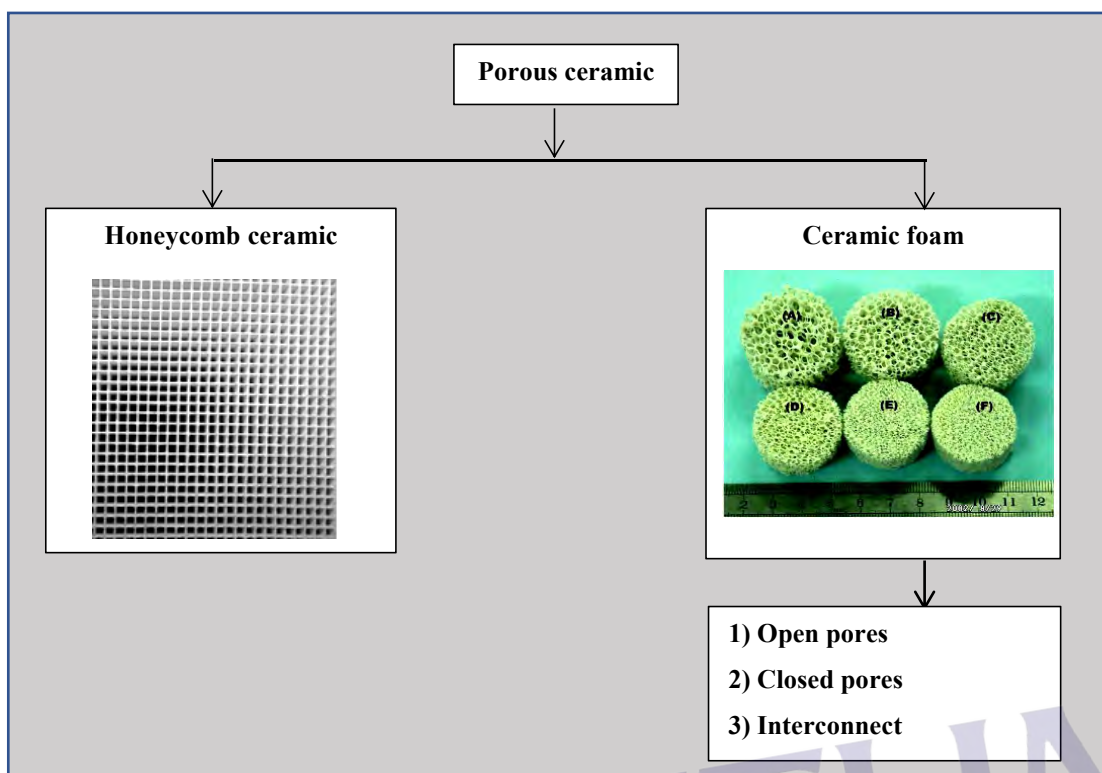


Figure 2.3: Type of porous ceramic (Al-Naib, 2018)

The common way to create ceramic honeycombs is extrusion molding, which involved mixing raw materials, extruding, drying, and firing to make the product. The ceramic honeycomb green body is obtained by extruding with the reticulated mold. After drying and sintering, porous ceramic honeycombs are produced with a regular shape. The green body has low strength, it is easily deformed, and surface dents and bubbles, cracks, and internal cracks may be found. Therefore, there are high requirements for compositions of the pug and property.

Solid open-cell foams have significantly higher mass and heat transfer coefficients compared with the monoliths and have a lower pressure drop relative to the packed bed. Ceramic foams are used as fused metal filters and thermal insulations at high temperatures (Gancarczyk *et al.*, 2019). Matching the catalytic output is necessary to understand the ceramic structure regarding porosity, pore size and mechanical strength. Table 2.1 shows the structure of the ceramic foams in previous studies.

Table 2.1: Structure of ceramic foam

Type of foam	Structure(s)	Reference
Ceramic foam	<ul style="list-style-type: none"> • Interconnected 	(Nasseh <i>et al.</i> , 2019)
Ceramic foam	<ul style="list-style-type: none"> • Open cell • Closed cell • Interconnected 	(Baharom <i>et al.</i> , 2018)
Ceramic foam	<ul style="list-style-type: none"> • Fully open • Closed cell • Interconnected 	(Rahim <i>et al.</i> , 2017)

Based on the studies in Table 2.1, an open ceramic foam is generated by the reticulated structures, where the solid species constituting the foamed body is comprised only of pore struts. When the pores are separated by solid cell walls, a closed-cell ceramic foam is achieved. The three-dimensional images of open cells and closed cells are as shown in Figure 2.4.

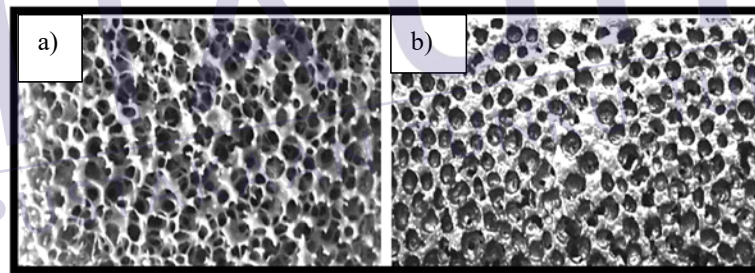


Figure 2.4: Three-dimensional images of ceramic foams: a) open pores and b) closed pores (Liu & Chen, 2014)

According to Wichianrat *et al.* (2012) and Ying *et al.* (2007), the open-cell foams refer to those with interpenetrating pores, while the closed-cell ones contain pores that are not interconnected. Typically, closed-cell foams exhibit relatively high compressive strength and therefore they are used in applications that require high strength and high energy absorption, such as automotive bumper and body armour applications. Figure 2.5 shows an example of a porous structure with some of the indicated features.

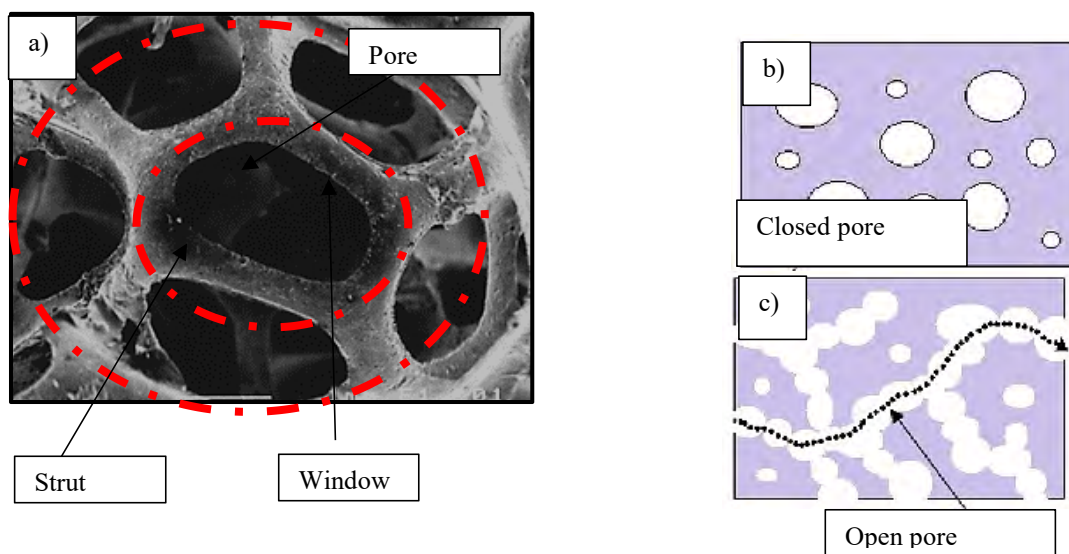


Figure 2.5: Examples of cells of ceramic foam: a) pore, window and strut, b) closed pores and c) open pores (Sampath *et al.*, 2016)

Porous ceramics also can be categorised according to the size of their pores, as shown in Table 2.2.

Table 2.2: Type of pores in ceramic foam

Type of pore	Size of pore
Microporous	< 2 nm
Mesoporous	2–50 nm
Macroporous	> 50 nm

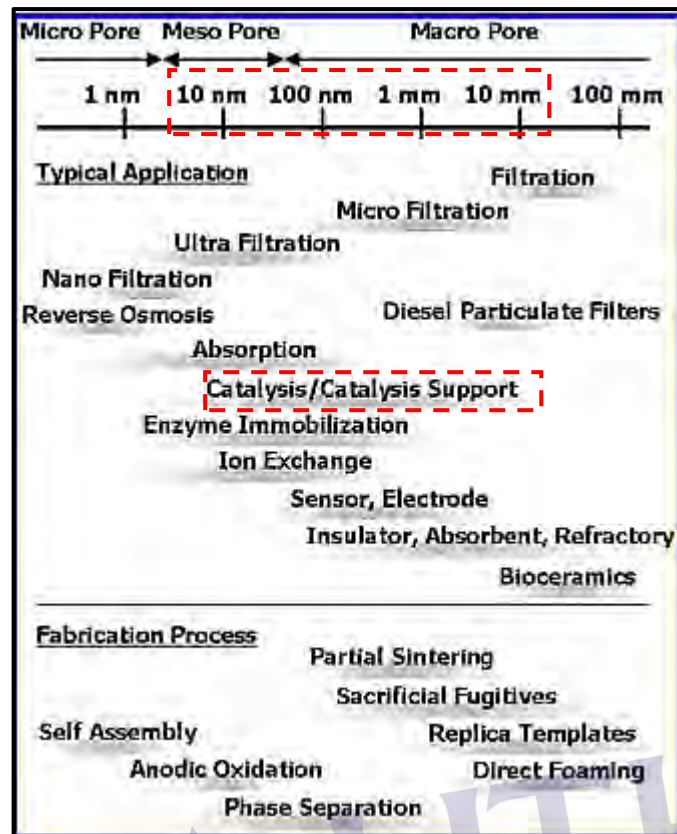


Figure 2.6: Schematic of classification of porous ceramics (Al-Naib, 2018)

Ahmad *et al.* (2014) studied porous materials and in their study, the selected starting ceramic powders were titanium dioxide (TiO_2), aluminium oxide (Al_2O_3) and silver nitrate (AgNO_3). In general, TiO_2 has lighter weight compared with other materials. Additionally, its brightness and refractive index are relatively high. On the other hand, Al_2O_3 is responsible for the resistance of metallic aluminium to weathering, while AgNO_3 plays an important role as antiseptics.

According to Buciuman & Czarnetzki (2003), ceramic foams can be extremely suitable catalytic carriers when a low-pressure drop is necessary. Compared with honeycomb monoliths, they offer additional advantages of radial mixing within the body and improved mass and heat transfer due to the turbulence of the flow.

2.6 Fabrication of Porous Material

Several processing methods have been investigated by researchers over the years to develop an open porous material that would have similar mechanical and physical properties to the gas catalyst. Importantly, the selection of the most suitable fabrication technique is based on the target application of the ceramic foam. This is due to the distinct properties of the ceramic foam produced by the manufacturing methods used and certain parameters involved, such as material selection, mixing, sintering temperature, sintering time and so on.

The fabrication technique can be classified according to the type of pores produced, which are open or closed pores, as illustrated in Figure 2.4. As previously mentioned, the selection of a suitable fabrication method is also based on the target application of the ceramic foam. In the present study, the structure of the ceramic foam as a gas catalyst (steam methane reforming) should consist of open and interconnected pores (Baharom *et al.*, 2018).

Currently, a majority of researchers use the direct foaming method, the replication method and the compaction method to produce the porous ceramic. At present, powder foaming at high temperature is the most effective approach to manufacture ceramic foams, especially the production of closed-pore ceramic foams (Xu *et al.*, 2010).

2.6.1 Foam replication method

The replication of polymer foams was one of the first manufacturing techniques developed for producing ceramics with controlled macroporosity, with the first patent acquired in 1963 by Schwartzwalder & Somers. Despite the modern era, it is still the most prevalent and commonly used method in the industry. In the replica technique, a cellular template is immersed or impregnated with a ceramic suspension/precursor solution to produce a porous ceramic having the same or different morphology as that of the original porous template. The replica method allows the fabrication of foams with larger porosity and pore size as well as being suitable for infrared heating applications (food processing) (Salleh *et al.*, 2019).

In recent years, corals, wood structures, eggshell membranes and bacteria have been used as natural templates. Open-pore structures in the range of 10 to 300 μm have been formed with this technique at porosity concentrations between 25% and 95%. The formation of a ceramic microstructure with anisotropic mechanical strength is one of these templates' shortcomings.

The replica method is one of the most significant manufacturing techniques for the fabrication of porous ceramics and is mainly used in the industry for the preparation of ceramic filters used in the filtration of liquid metals and other helpful applications. The sponge replica technique is a novel technique. The essential steps in this process include the adhesion of the suspension on the polymeric sponge and the rheology of the slurry. Due to high pore interconnectivity, the permeability of gasses and fluids is enhanced in these porous materials. Despite being a user-friendly process, cellular structures processed through this route have deficient mechanical strength due to the formation of cracked struts at the time of polymer sponge pyrolysis (Studart *et al.*, 2006). However, by not involving any hazardous chemicals in the process, this method is the simplest and cheapest process to use (Ahmad *et al.*, 2016)

Many distinct polymers may be used in this technique for foam precursors, including polyurethane (PU), polyvinyl chloride (PVC), polystyrene (PS) and cellulose. Selee Corp. in the USA, for instance, utilises an interconnected, open-cell polyurethane foam with a 97% vacuum volume as an organic precursor, the design of which consists of a complicated pattern of dodecahedra repeated in three dimensions. In addition, the PU foam used is also inexpensive, readily available and has a uniform microstructure (Tange *et al.*, 2015). In this method, the PU foam is usually used as a sacrificial template due to its microstructure, which is typically similar to the microstructure of a filter catalyst, as shown in Figure 2.7. The replication method involves a three-step replication process, as shown in Figure 2.8.

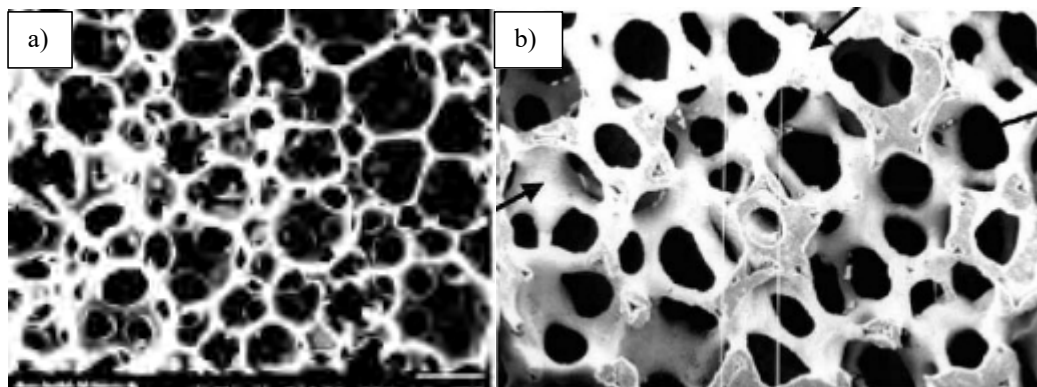


Figure 2.7: Microstructure of a) PU foam template (Asadi & Ohadi, 2015) and b) ceramic filter catalyst (Twigg & Richardson, 2002)

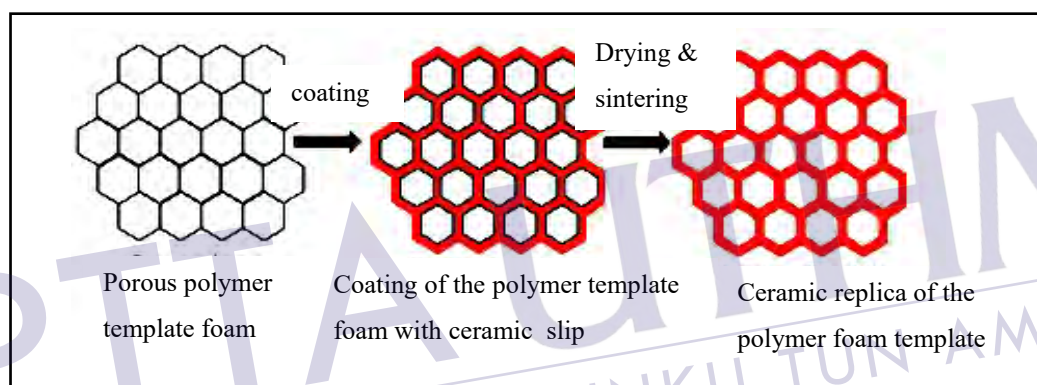


Figure 2.8: Schematic of porous material fabrication via the replication method (Bowen & Thomas, 2015)

Usually, the PU foam is initially immersed in a slurry containing metallic particles and suitable binders before subsequently being dried. After that, the PU template and the binders will be removed by pyrolysis, followed by sintering, which produces a reticulated open-cell foam (Ryan *et al.*, 2006). Generally, pyrolysis is a thermal decomposition process to eliminate the binders and the PU foam template. The temperature for the pyrolysis process mainly depends on the type of binders and the PU foam used, since both have different decomposition temperatures. However, in the replica foam method, due to the cracking of the struts during pyrolysis, the mechanical properties of the reticulated foams are generally poor.

Fey *et al.* (2017) reported that it is crucial to determine the decomposition temperatures of the binders and the PU foam used. The decomposition temperatures can be identified by using thermogravimetric analysis (TGA). The samples' strength

during and after the pyrolysis process is very fragile since the powder particles are only loosely connected and are not sintered yet. In addition, a lower heating rate is favoured to avoid thermal and mechanical stress generation due to the thermal expansion mismatch between the PU foam and the metal powder coating, which will cause defect formation or cracked struts (Studart *et al.*, 2006). Usually, the pyrolysis process is carried out at about 1 hr of dwell time to allow sufficient time for the complete removal of the binders and the PU foam (Tange *et al.*, 2015).

The replication method is done by the slurry method. According to a study by Mishra *et al.* (2009), the advantage of the slurry-based processing is the uniform distribution of the various phases through the co-dispersion in a solvent. Kovářik *et al.* (2017) used a ten-pore-per-inch polyurethane foam as a template, which was infiltrated with an aqueous potassium-based geopolymer slurry, obtaining a geopolymer/polyurethane porous composite after the drying step. Cellular geopolymers with a large amount of open porosity (~79 to ~88 vol%) and reasonably good compressive strength (~0.15 to ~0.85 MPa) were produced after sintering at 1100°C–1300°C for 4 hr.

Baharom *et al.* (2018.) reported that the replication method affects the size and distribution of the open and closed pores and the size of struts which connect the cell windows together. Mishra *et al.* (2009) reported that the results of the microstructural and mercury porosimetry studies of the composite foams showed a trimodal size distribution with small (4 nm to 8 μ m), medium (40 μ m to 200 μ m) and large (\approx 1 mm or more) pores. The pores appeared spherical and interconnected, with the fibres embedded in the cell walls or struts.

As reported by Wen *et al.* (2008), the impregnation of polymeric sponge into slurries containing particles and appropriate binders was followed by drying and sintering. The porous ceramics produced by this method have open-cell structures. However, one of the more attractive features of this method lies in the easy control of the pore size by choosing different sponge templates, which is the main reason for the wide application of this method in the industry. The porous ceramics produced have open cells with porosity of around 74% to 78%.

Diverse types of porous materials have been successfully developed using the replication method, as summarised in Table 2.3 and Table 2.4. The scanning electron microscopy (SEM) images observed in Table 2.4 show that most porous materials produced by this method consist of open and interconnected pores. Indeed, porosity

REFERENCES

- Abdullah, Z. (2015). *Fabrication of 316l stainless steel (ss316l) foam via powder compaction method*, Universiti Tun Hussein Onn Malaysia, Degree of Master
- Ahmad, S., Halim, N. H., Taib, H., & Harun, Z. (2014). Effect of sintering temperature on the physical properties of titania- alumina-silver nitrate foam. *Applied Mechanics and Materials*, 465–466, 877–880.
- Ahmad, S., & Kassim, A. (2011). Fabrication of titanium foam by using compaction method. *Eprints.Uthm.Edu.My*.
- Ahmad, S., Latif, M. A., Taib, H., & Ismail, A. F. (2013). Short Review: Ceramic Foam Fabrication Techniques for Wastewater Treatment Application. *Advanced Materials Research*, 795, 5–8.
- Ahmad, S., Rosli, M., Abdul Manaf, N. S., Mahammad Rafter, M. F., & Nor, M. F. (2016). The formation of cobalt chromium molybdenum (CoCrMo) foams fabricated by slurry method. *Materials Science Forum*, 840, 197–201.
- Al-Naib, U. M. B. (2018). Introductory Chapter 1: A Brief Introduction to Porous Ceramic. *Recent Advances in Porous Ceramics*, 1–10.
- Al-Swai, B. M., Osman, N. B., & Abdullah, B.(2017). Catalytic performance of Ni/MgO catalyst in methane dry reforming. In *AIP Conference Proceedings* 1891, pp. 1–7.
- Al, M., Muhamad, A., Chain, L., Arifin, Z., & Akil, H. (2008). Preparation and characterization of ceramic foam produced via polymeric foam replication method. *Journal of Materials Processing Technology*, 7(207), 235–239.

- Altunal, V., Guckan, V., Ozdemir, A., Sotelo, A., & Yegingil, Z. (2019). Effect of sintering temperature on dosimetric properties of BeO ceramic pellets synthesized using precipitation method. *Nuclear Instruments and Methods in Physics Research, Section B: Beam Interactions with Materials and Atoms*, 441, 46–55.
- Asadi, M., & Ohadi, A. (2015). Improving Sound Absorption of Polyurethane Foams By the Incorporation of Nano-Particles. *The 22nd International Congress on Sound and Vibration*, 22(July), 12–16.
- Azancot, L., Bobadilla, L. F., Santos, J. L., Córdoba, J. M., Centeno, M. A., & Odriozola, J. A. (2019). Influence of the preparation method in the metal-support interaction and reducibility of Ni-Mg-Al based catalysts for methane steam reforming. *International Journal of Hydrogen Energy*, 44(36), 19827–19840.
- Azmi, M. A., Ismail, N. A. A., Rizamarhaiza, M., Hasif, A. A. K. W. M., & Taib, H. (2016). Characterisation of silica derived from rice husk (Muar, Johor, Malaysia) decomposition at different temperatures. *AIP Conference Proceedings*, 1756, 02005–1. 48
- Baharom, S. (2014). *Chapter 2*. Universiti Tun Hussein Onn Malaysia, Degree of Master
- Baharom, S., Ahmad, S., Taib, H., & Muda, R. (2016). The effects of composition and sintering temperature on the silica foam fabricated by slurry method. In *American Institute of Physics*. 1756, 020004.
- Baharom, S., Ahmad, S., & Taib, H. (2018). Morphological Analysis of Silica-Nickel Oxide Foam Fabricated by Replication Method. *International Journal Of Current Science, Engineering & Technology*, 396–402.
- Bakar, R.A., Yahya, R., & Gan, S. N. (2016). Production of high purity amorphous silica from rice husk. *Procedia Chemistry*, 19, 189–195.



- Barakat, A., Al-Noaimi, M., Suleiman, M., Aldwayyan, A. S., Hammouti, B., Hadda, T. Ben., & Warad, I. (2013). One step synthesis of NiO nanoparticles via solid-state thermal decomposition at low-temperature of novel aqua(2,9-dimethyl-1,10-phenanthroline) NiCl_2 complex. *International Journal of Molecular Sciences*, 14(12), 23941–23954.
- Bej, B., Pradhan, N.C., & Neogi, S.(2013). Production of hydrogen by steam reforming of methane over alumina supported nano-NiO/SiO₂ catalyst. *Catalysis Today*, 207, 28–35.
- Belhadi, A., Boumaza, S., Djadoun, A., Trari, M., & Cherifi, O. (2016). Methane steam reforming on supported nickel , effect of nickel content for product hydrogen. *Journal of Physical Chemistry*, 6, 34–41.
- Bertolla, L., Chlup, Z., Tatarko, P., Hanzel, O., Sevecek, O., Roupцова, P., & Dlouhy, I. (2018). Preparation and characterization of novel environmentally friendly $\text{Al}_2\text{O}_3/\text{SiO}_2/\text{CaO}$ ceramic foams. *Ceramics International*, 44(15), 19063–19069.
- Beurden, P. V.(2004). On the catalytic aspects of steam-methane reforming a *Literature Survey*. 12,1-27
- Bie, R. S., Song, X. F., Liu, Q. Q., Ji, X. Y., & Chen, P. (2015). Studies on effects of burning conditions and rice husk ash (RHA) blending amount on the mechanical behavior of cement. *Cement and Concrete Composites*, 55, 162–168.
- Boudjeloud, M., Boulahouache, A., Rabia, C., & Salhi, N. (2019). La-doped supported Ni catalysts for steam reforming of methane. *International Journal of Hydrogen Energy*, 44(20), 9906–9913.
- Bowen, C. R., & Thomas, T. (2015). Macro-porous Ti_2AlC MAX-phase ceramics by the foam replication method. *Ceramics International*, 41(9), 12178–12185.
- Buciuman, F.C., & Kraushaar-Czarnetzki, B. (2003). Ceramic foam monoliths as catalyst carriers. Adjustment and description of the morphology. *Industrial and Engineering Chemistry Research*, 42(9), 1863–1869.



Carcinogen, S. H. (2006). *Silica , Crystalline : A -Quartz and Cristobalite*.

Chai, R., Zhang, Z., Chen, P., Zhao, G., Liu, Y., & Lu, Y. (2017). Ni-foam-structured NiO-MO_x-Al₂O₃ (M = ¼ Ce or Mg) nanocomposite catalyst for high throughput catalytic partial oxidation of methane to syngas. *Microporous and Mesoporous Materials*, 253, 123–128.

Chandrasekhar, S., Satyanarayana, K. G., Pramada, P. N., Raghavan, P., & Gupta, T. N. (2003). Review Processing, properties and applications of reactive silica from rice husk-an overview. *Journal Of Materials Science*. 38, 3159-3168

Che Daud, Z., & Jamaludin, S. B. (2013). The Effect of Sintering on the Properties of Powder Metallurgy (PM) F-75 Alloy. *Advanced Materials Research*, 795, 573–577.

Chen, A. N., Li, M., Xu, J., Lou, C. H., Wu, J. M., Cheng, L. J., & Li, C. H. (2018). High-porosity mullite ceramic foams prepared by selective laser sintering using fly ash hollow spheres as raw materials. *Journal of the European Ceramic Society*, 38(13), 4553–4559.

Chen, P., Kim, G. Y., & Ni, J. (2007). Investigations in the compaction and sintering of large ceramic parts. *Journal of Materials Processing Technology*, 190 (1–3), 243–250.

Cheng, W., Wang, Z., Ren, C., Chen, H., & Tang, T. (2007). Preparation of silica/polyacrylamide/polyethylene nanocomposite via in situ polymerization. *Materials Letters*, 61(14–15), 3193–3196.

Choi, H. J., Kim, J. U., Kim, H. S., Kim, S. H., & Lee, M. H. (2015). Ceramics Effect of sintering temperature in preparation of granular ceramic filter. *Ceramics International*, 41, 10030–10037.

D'Amico, G. (2015). *Si-SiC based materials obtained by infiltration of silicon: study and applications*. Politecnico di Torino Dipartimento Scienza Applicata e Tecnologia (DISAT), Ph.D thesis



- Dalgleish, T., Williams, J. M. G., Golden, A. M. J., Perkins, N., Barrett, L. F., Barnard, P. J., & Watkins, E. (2007). *A Compact and Efficient Steam Methane Reformer for Hydrogen Production*, University of Houston. Ph.D thesis.
- Darda, S., Pachatouridou, E., Lappas, A., & Iliopoulou, E. (2019). Effect of Preparation Method of Co-Ce Catalysts on CH₄ Combustion. *Catalysts*, 9 (3), 219.
- Dehaghani, M. T., & Ahmadian, M. (2015). Effect of sintering temperature and time on the mechanical properties of Co-Cr-Mo/58S bioglass porous nano-composite. *Bulletin of Materials Science*, 38 (5), 1239–1246.
- Della, V. P., Kuhn, I., & Hotza, D. (2002). Rice husk ash as an alternate source for active silica production. *Materials Letters*, 57, 818–821.
- Deshmukh, P., Bhatt, J., Peshwe, D., & Pathak, S. (2012). Determination of silica activity index and XRD, SEM and EDS studies of amorphous SiO₂ extracted from rice Husk Ash. *Transactions of the Indian Institute of Metals*, 65(1), 63–70.
- Duan, B., Shen, T., & Wang, D. (2019). Effects of solid loading on pore structure and properties of porous FeAl intermetallics by gel casting. *Powder Technology*, 344, 169–176.
- Emadwiandr. (2013). *Current Developments in Biotechnology and Bioengineering: Resource Recovery*. United States: Elsevier
- Falliano, D., Domenico, D. De, Ricciardi, G., & Gugliandolo, E. (2018). Experimental investigation on the compressive strength of foamed concrete : Effect of curing conditions , cement type , foaming agent and dry density. *Construction and Building Materials*, 165, 735–749.
- Fang, X., Zhang, X., Guo, Y., Chen, M., Liu, W., Xu, X., & Gao, Z. (2016). ScienceDirect Highly active and stable Ni / Y₂Zr₂O₇ catalysts for methane steam reforming : On the nature and effective preparation method of the pyrochlore support. *International Journal of Hydrogen Energy*, 41(26), 11141–11153.



PTT A UTHM
PERPUSTAKAAN TUNKU TUN AMINAH

- Fernandes, I. J., Calheiro, D., Sanchez, F. A. L., Luisa, A., Camacho, D., Avila, D. C. R. T. L., & Caldas, D. S. V. (2017). Characterization of silica produced from rice husk ash: Comparison of purification and processing methods. *Materials Research*, 20, 512–518.
- Gancarczyk, A., Sindera, K., Iwaniszyn, M., Piątek, M., Macek, W., Jodłowski, P. J., & Kołodziej, A. (2019). Metal foams as novel catalyst support in environmental processes. *Catalysts*, 9(7), 587.
- Galvan, A. C., Melian, M., Ruiz-Matas, L., Eslava, J. L., Navarro, R. M., Ahmadi, M., & Fierro, J. L. G. (2019). Partial oxidation of methane to syngas over nickel-based catalysts: Influence of support type, addition of rhodium, and preparation method. *Frontiers in Chemistry*, 7, 1–16.
- Ghazali, M. S. M., Shaifudin, M. S., Abdullah, W. R. W., Kamaruzzaman, W. M. I. W. M., Fekeri, M. F. M., & Zulkifli, M. A. (2018). Conventional sintering effects on the microstructure and electrical characteristics of low-voltage ceramic varistor. In *Sintering Technology - Method and Application*, 65–82.
- Guan, K., Qin, W., Liu, Y., Yin, X., Peng, C., Lv, M., & Wu, J. (2016). Evolution of porosity, pore size and permeate flux of ceramic membranes during sintering process. *Journal of Membrane Science*, 520, 166–175.
- Han, Y. S., Li, J. B., & Chen, Y. J. (2003). Fabrication of bimodal porous alumina ceramics. *Materials Research Bulletin*, 38, 373–379.
- Han, Y. S., Li, J. B., Chen, Y. J., & Wei, Q. M. (2002). A study on the factors involved in collapse of macroporous $\text{-Al}_2\text{O}_3$ structure. *Journal of Materials Processing Technology*, 128(1–3), 313–317.
- Han, Y., Wen, B., & Zhu, M. (2017). Excellent catalytic performance for syngas methanation reactions. *Catalysts*, 7 (21), 1–11.
- Haslinawati, M. M., Matori, K., Wahab, Z., Sidek, H., & Zainal, T. (2009). Effect of temperature on ceramic from rice husk ash. *International Journal of Basic & Applied Sciences*, 09(09), 1985–1988.



- Hermawan, H., Dube, D., & Mantovani, D. (2010). Developments in metallic biodegradable stents. *Acta Biomaterialia*, 6(5), 1693–1697.
- Higginson, R. L., Jackson, C. P., Murrell, E. L., Exworthy, P. A. Z., Mortimer, R. J., Worrall, D. R., & Wilcox, G. D. (2015). Effect of thermally grown oxides on colour development of stainless steel. *Materials at High Temperatures*, 32 (1–2), 113–117.
- Hossain, S. K. S., Mathur, L., & Roy, P. K. (2018). Rice husk/rice husk ash as an alternative source of silica in ceramics: A review. *Journal of Asian Ceramic Societies*, 6 (4), 299–313
- Huo, W., Zhang, X., Chen, Y., Lu, Y., Liu, J., Yan, S., & Yang, J. (2017). Novel mullite ceramic foams with high porosity and strength using only fly ash hollow spheres as raw material. *Journal of the European Ceramic Society*, 1–8.
- Hwang, S. S., & Hsu, P. P. (2013). Effects of silica particle size on the structure and properties of polypropylene/ silica composites foams. *Journal of Industrial and Engineering Chemistry*, 19, 1377–13883.
- Iatsenko, A., Sych, O., & Tomila, T. (2015). Effect of sintering temperature on structure and properties of highly porous glass-ceramics. *Processing and Application of Ceramics*, 9 (2), 99–105
- Ossi, I. C. D. (2016). Potassium oxide analysis in rice husk ash at various combustion conditions using proton-induced X-Ray Emission (PIXE) spectrometric technique. *International Journal of Applied Chemistry*, 12 (3), 281–291.
- J, R. P., W, M. A., Z, M, S. M., H, A. B. B., Johari A, M. M., & Ibrahim H, W. M. (2012). Thermal Analysis and Pozzolanic Index of Rice Husk Ash at Different Grinding Time. *Procedia Engineering*, 00, 1-9
- Jaafar, C. N. A., Zainol, I., Sulaiman, S., & Ayub, M. I. (2014). Effects of PVA-PEG binders system on microstructure and properties of sintered alumina. *Applied Mechanics and Materials*, 564, 355–360.

- Jamil, M., Khan, M. N. N., Karim., M. R., Kaish, A. B. M. A., & Zain, M. F.M. (2016). Physical and chemical contributions of Rice Husk Ash on the properties of mortar. *Construction and Building Materials*, 128, 185-198
- Jasik, A., Wojcieszak, R., Monteverdi, S., Ziolk, M., & Bettahar, M. M. (2005). Study of nickel catalysts supported on Al_2O_3 , SiO_2 or Nb_2O_5 oxides. *Journal of Molecular Catalysis A: Chemical*, 242, 81–90.
- Jeanmonod, D. J., Rebecca, & Suzuki, K. (2018). *Advanced Ceramic Processing: Porous Ceramic*. Intech Open, 2, 64.
- Ji, C., He, D., Shen, L., Zhang, X., Wang, Y., Gupta, A., & Bao, N. (2014). A facile green chemistry route to porous silica foams. *Materials Letters*, 119, 60–63.
- Jia, C., Liu, J., Ding, R., Teng, D., & Feng, L. (2016). Effects of the sintering temperature on the structure and properties of the alumina foamed ceramics. *MATEC Web of Conferences*, 67, 67.
- Kalapathy, U., Proctor, A., & Shultz, J. (2000). A simple method for production of pure silica from rice hull ash. *Bioresource Technology*, 73, 257–262.
- Kemary. M., Nagy, N., & El-Mehasseb, I. (2003), Nickel oxide nanoparticles: Synthesis and spectral studies of interactions with glucose. *Materials Science in Semiconductor Processing*, 6, 1747-1752
- Kavitha, B., Nirmala, M., & Pavithra, A. (2016). Annealing effect on nickel oxide nanoparticles synthesized by sol-gel method. *World Scientific News*, 52, 118–129.
- Kim, H., Lee, S., Han, Y., & Park, J. (2009). Control of pore size in ceramic foams: Influence of surfactant concentration. *Materials Chemistry and Physics*, 113(1), 441–444
- Kovarik, T., Krenek, T., Rieger, D., Pola, M., Riha, J., Svoboda, M., & Kadlec, J. (2017). Synthesis of open-cell ceramic foam derived from geopolymer precursor via replica technique. *Materials Letters*, 209, 497-500
- Kumar, S., Sangwan, P., V, D. R. M., & Bidra, S. (2013). Utilization of rice husk and their ash: A Review. *Journal of Chemical and Environmental Sciences*, 1(5), 126–129.



- Kusakabe, K., Sotowa, K. I., Eda, T., & Iwamoto, Y. (2004). Methane steam reforming over Ce-ZrO₂-supported noble metal catalysts at low temperature. *Fuel Processing Technology*, 86 (3), 319–326.
- Larbi, K. K. (2010). *Synthesis of High Purity Silicon from Rice Husks*. University of Toronto, Degree of Master
- Li, B., Qian, X., & Wang, X. (2015). Oxidative CO₂ reforming of methane over stable and active nickel-based catalysts modified with organic agents. *International Journal of Hydrogen Energy*, 40 (25), 8081–8092.
- Li, F., Kang, Z., Huang, X., Wang, X. G., & Zhang, G. J. (2014). Preparation of zirconium carbide foam by direct foaming method. *Journal of the European Ceramic Society*, 34(15), 3513–3520.
- Li, P., Chen, L., Xia, S., Zhang, L., Kong, R., Ge, Y., & Feng, H. (2020). Entropy generation rate minimization for steam methane reforming reactor heated by molten salt. *Energy Reports*, 6, 685–697.
- Li, Z., Hu, X., Zhang, L., Liu, S., & Lu, G. (2012). Steam reforming of acetic acid over Ni/ZrO₂ catalysts: Effects of nickel loading and particle size on product distribution and coke formation. *Applied Catalysis A: General*, 417–418, 281–289.
- Liang, Y., Liu, Q., Asiri, A. M., Sun, X., & He, Y. (2015). Nickel–iron foam as a three-dimensional robust oxygen evolution electrode with high activity. *International Journal of Hydrogen Energy*, 5–10.
- Liu, J. A. (2006). *Kinetics, catalysis and mechanism of methane steam reforming of Science in Chemical Engineering*. Worcester Polytechnic Institute, Degree of Master
- Liu, P. S., & Chen, G. F. (2014). General introduction to porous materials. *Porous Materials*, 1–20.
- Liu, Y., Duan, D. L., Jiang, S. L., & Li, S. (2015). Preparation and its cavitation performance of nickel foam/epoxy/SiC co-continuous composites. *Wear*, 332–333, 979–987.



PT TUN AMINAH
PERPUSTAKAAN

- Liu, Y, Guo, Y., Gao, W., Wang, Z., Ma, Y., & Wang, Z. (2012). Simultaneous preparation of silica and activated carbon from rice husk ash. *Journal of Cleaner Production*, 32, 204–209.
- Liu, S., Zeng, W., & Chen, T. (2016). Synthesis of hierarchical flower-like NiO and the influence of surfactant. *Physica*, 85, 13–18.
- Ma, B., Li, Y., Liu, G., & Liang, D. (2015). Preparation and properties of Al₂O₃–MgAl₂O₄ ceramic foams. *Ceramics International*, 41(2), 3237–3244.
- Madon, H. R., Fawzi, M., Ilman, S. K., Osman, A. S., Razali, A. M., & Mohammad, W. A. (2018). Effect of reaction temperature on steam methane reforming's yield over coated nickel aluminide (Ni₃Al) catalyst in micro reactor. *Journal of Advanced Research in Fluid Mechanics and Thermal Sciences Journal Homepage*, 50, 170–177.
- Madon, R. H., Sarwani, M. K. I., Fawzi, M. (2016). Effect of substrate surface roughness on morphological and topography of nickel-alumina thin film. *ARPN Journal of Engineering and Applied Sciences*, 8, 5304–5308.
- Majewski, A. J., Wood, J., & Bujalski, W. (2013). Nickel-silica core@shell catalyst for methane reforming. *International Journal of Hydrogen Energy*, 38(34), 14531–14541.
- Manonukul, A., Tange, M., Srikudvien, P., Denmud, N., & Wattanapornphan, P. (2014). Rheological properties of commercially pure titanium slurry for metallic foam production using replica impregnation method. *Powder Technology*, 266, 129–134.
- Mao, X., Wang, S., & Shimai, S. (2006). Porous ceramics with tri-modal pores prepared by foaming and starch consolidation. *Ceramics International*, 34(34), 107–112.
- Matos, M. J., Dias, S., & Oliveira, F. A. C. (2007). Macrostructural changes of polymer replicated open cell cordierite based foams upon sintering. *Advances in Applied Ceramics*, 106(5), 209–215.



- Mat, N. F., Jamaludin, K. R., & Ahmad, S. (2017). Fabrication of porous stainless Steel 316L for biomedical applications. *MATEC Web of Conferences*, 135, 1–7
- Mat, N. F, Bakar, A. M. I., Mohamad, Z., Ismail, A. E., Ismon, M., Ahmad, S., & Sanusi, S. H. (2019). Composition and type of a binder effects on the stainless steel foam microstructure prepared by sponge replication method. *International Journal of Integrated Engineering*, 11(7), 90–94.
- Meloni, E., Martino, M., & Palma, V. (2020). A short review on ni based catalysts and related engineering issues for methane steam reforming. *Catalysts*, 10(3).
- Ming, Q., Healey, T., Allen, L., & Irving, P. (2002). Steam reforming of hydrocarbon fuels. *Catalysis Today*, 77(1–2), 51–64.
- Ministry of Energy Green Technology and Water. (2017). *Green Technology Master Plan Malaysia 2017 - 2030*.
- Mishra, S., Mitra, R., & Vijayakumar, M. (2009). Processing and microstructure of particle stabilized silica foams. *Materials Letters*, 63(30), 2649–2651.
- Mohammadyani, D., Hosseini, S., & Sadrnezhad, S. K. (2012). Characterization of nickel oxide nanoparticles synthesized via rapid microwave-assisted route. *International Journal of Modern Physics: Conference Series*, 05, 270–276.
- Moosa, A. A., & Saddam, B. F. (2017). Synthesis and characterization of nanosilica from rice husk with applications to polymer composites. *American Journal of Materials Science*, 7(6), 223–231.
- Mousavi, S. E., & Karamvand, A. (2017). Assessment of strength development in stabilized soil with CBR PLUS and silica sand. *Journal of Traffic and Transportation Engineering (English Edition)*, 4(4), 412–421.
- Music, S., Vincekovic, F. N., & Sekovanic, L. (2011). Precipitation of amorphous SiO₂ particles and their properties. *Journal of Chemical Engineering*, 28, 89–94



- Naceur, H., Megriche, A., & El Maaoui, M. (2014). Effect of sintering temperature on microstructure and electrical properties of $\text{Sr}_{1-x}(\text{Na}_{0.5}\text{Bi}_{0.5})_x\text{Bi}_2\text{Nb}_2\text{O}_9$ solid solutions. *Journal of Advanced Ceramics*, 3(1), 17–30.
- Nasseh, S., Mehranbod, N., & Eslamloueyan, R. (2019). Optimization of ceramic foam fabrication for removal of aluminium ion from aqueous solutions. *Journal of Environmental Chemical Engineering*, 7(6), 103513.
- Nazaruddin, N, A., Rahim, P. S. A., M. R., K, W. M. H. A., Azmi, M. A., Taib, H., & Ahmad, S. (2017). The effect of different binder compositions in fabricating silica foam (SiO_2) via replication method. *Journal of Mechanical Engineering*, 4(5), 53–62.
- Ni, S., Lv, X., Ma, J., Yang, X., & Zhang, L. (2014). A novel electrochemical reconstruction in nickel oxide nanowalls on Ni foam and the fine electrochemical performance as anode for lithium ion batteries. *Journal of Power Sources*, 270, 564–568.
- Nor, M. A. A. M., Akil, H. M., & Ahmad, Z. A. (2009). The effect of polymeric template density and solid loading on the properties of ceramic foam. *Science of Sintering*, 41, 319–327.
- Omar, A. M., & Subuki, I. (2012). Sintering - Methods and Products. In *Sintering - Methods and Products*, 127–146.
- Onojah, A.D., Agbendeh, N. A., & Mbakaan, C. (2013). Rice husk ash refractory : The temperature dependent crystalline phase aspects. *Ijrras*, 15(2), 246–248
- Ossi, C. D. I. (2016). Potassium oxide analysis in rice husk ash at various combustion conditions using proton-induced X-ray emission (PIXE) spectrometric technique. *International Journal of Applied Chemistry*, 12, 281 -291
- Ozdemir, H., Oksuzomer, M. A. F., & Gurkaynak, M. A. (2010). Preparation and characterization of Ni based catalysts for the catalytic partial of methane : Effect of support basicity on H_2/CO ratio and carbon deposition. *International Journal of Hydrogen Energy*, 35, 12147-12160



PTTA UTHM
PUSAT TEKNOLOGI DAN TERAPI AKADEMIK
UNIVERSITI TEKNIKAL MALAYSIA MELAKA

- Pierozynski, B., Mikolajczyk, T., & Kowalski, I. M. (2014). Hydrogen evolution at catalytically-modified nickel foam in alkaline solution. *Journal of Power Sources*, 271, 231–238.
- Rahman, H. A., & Guan, Y. C. (2007). Preparation of ceramic foam by simple casting process. *International Conference on Engineering and Environment*, 2-5
- Rahman, H. A., & Yacob, D. H. (2008). Effects of double sintering on the properties of porous ceramic. *UTHM, Institutional Repository*, 1–6.
- Rahaman, M. N., & Dekker, M. (2013). Sintering stages
- Rahim, P. S. A., & Shamsudin, M. S., M. R., Nazaruddin, N. A., Azmi, M. A., Mahzan, S., Ahmad, S., & Taib, H. (2017). The effect of nickel oxide (NiO) compositions in consolidation of silica- foams using replication method. *Journal of Mechanical Engineering*, 4(5), 63–72.
- Ren, X., Ma, B., Zhang, Y., Zhu, Q., Li, D., Li, S., & Li, H. (2018). Effects of sintering temperature and V_2O_5 additive on the properties of SiC- Al_2O_3 ceramic foams- $Al_2O_3V_2O_5$ sintering porosity strength polymeric foam replication method. *Journal of Alloys and Compounds*, 732, 716–724.
- Rifaya, M. N., Theivasanthi, T., & Alagar, M. (2012). Chemical capping synthesis of nickel oxide nanoparticles and their characterizations studies. *Nanoscience and Nanotechnology*, 2(5), 134-138
- Rosip, M, N. I., Ahmad, S., Arpawi, N. L., Jamaluddin, K. R., & Mat, N. F. (2014). The effect of sintering temperature and composition for density and porosity of SS316L foam. *Applied Mechanics and Materials*, 465–466, 988–992.
- Ryan, G., Pandit, A., & Āpatsidis D. P, (2006). Fabrication methods of porous metals for use in orthopaedic applications. *Biomaterial*, 27, 2651–2670.
- Salleh, N. A., Ab Hamid, K., Mohd Naw, M. N., & Abd. Mutalib, S. (2019). Improving safety culture: Positive environmental impacts of information delivery to foreign workers. *Ekoloji*, 28(107), 123–127.

- Sampath, U. G. T. M., Ching, Y. C., Chuah, C. H., Sabariah, J. J., & Lin, P. C. (2016). Fabrication of porous materials from natural/synthetic biopolymers and their composites. *Materials*, 9 (12), 1–32.
- Sankar, S., Sharma, S. K., Kaur, N., Lee, B., Kim, D. Y., Lee, S., & Jung, H. (2016). Biogenerated silica nanoparticles synthesized from sticky, red, and brown rice husk ashes by a chemical method. *Ceramics International*, 42(4), 4875–4885.
- Saxena, S. (2004). Chemical and technical assessment (CTA) 61st JECFA - Polyvinyl alcohol (PVA). *Chemical and Technical Assessment*, 1(3), 1–3.
- Seraj, S., Cano, R., Ferron, R. D., & Juenger, M. C. G. (2017). The role of particle size on the performance of pumice as a supplementary cementitious material. *Cement and Concrete Composites*, 80, 135–142.
- Sobrosa, F., Stochero, N., & Marangon, E. (2017). Development of refractory ceramics from residual silica derived from rice husk ash. *Ceramics International*, 43, 7142–7146.
- Speight, J. G. (2015). *Gasification processes for syngas and hydrogen production. Gasification for Synthetic Fuel Production: Fundamentals, Processes and Applications*. United State, 119-146
- Studart, A. R., Gonzenbach, U. T., Tervoort, E., & Gauckler, L. J. (2006). Processing routes to macroporous ceramics: A Review. *Journal of the American Ceramic Society*, 89(6), 1771–1789.
- Syamimi, N. F., Amin, M, K., Lim, W. F., Aziz, A, S., & Zaid, M. H. M. (2014). Effect of sintering temperature on structural and morphological properties of europium (III) oxide doped willemite. *Journal of Spectroscopy*, 2014, 1–9.
- Taghizadeh, M. T., & Sabouri, N. (2013). Thermal degradation behavior of Polyvinyl Alcohol / Starch / Carboxymethyl Cellulose / Clay Nanocomposites. *Universal Journal of Chemistry*, 1(2), 21–29.
- Taib. M. R. (2007). *Production Of Amorphous Silica From Rice Husk In Fluidised Bed System*. Universiti Teknologi Malaysia, Research vot



- Tange, M., Manonukul, A., & Srikudvien, P. (2015). The effects of organic template and thickening agent on structure and mechanical properties of titanium foam fabricated by replica impregnation method. *Materials Science & Engineering*, 641, 54–61.
- Tatt, T. K., Muhamad, N., Muchtar, A., Sulong, A. B., & Cherng, N. M. (2016). Influence of sintering parameters on the compressive yield strength of stainless steel foams produced by the space holder method. *Sains Malaysiana*, 45(4), 653–658.
- Taufik, R. S., Adibah, N. F. M., Muhamad, M. R., & Hasib, H. (2013). Feasibility study of natural fiber composite material for engineering application. *Journal of Mechanical Engineering and Sciences (JMES)*, 6, 1–3.
- Temkin, M. I. (1979). *The Kinetics of Some Industrial Heterogeneous Catalytic Reactions*. Moscow. Advances in Catalysis (Vol. 28).
- Tripkovic, D., Radojevic, V., & Aleksic, R. (2006). Factors affecting the microstructure of porous ceramics. *Journal of the Serbian Chemical Society*, 71(3), 277–284.
- Twigg, M. V., & Richardson, J. T. (2002). Theory and applications of ceramic foam catalysts. *Chemical Engineering Research and Design*, 80 (2), 183–189.
- Vilcekova, Z., Kasiarova, M., Domanicka, M., Hnatko, M., & Sajgalik, P. (2013). Influence of the preparation of Si_3N_4 based foams on the compressive strength and processing flaws. *Powder Metallurgy Progress*, 13, 139–146.
- Wang, L., Lu, A., Wang, C., Zheng, X., Zhao, D., & Liu, R. (2006). Nano-fibriform production of silica from natural chrysotile. *Journal of Colloid and Interface Science*, 295(2), 436–439.
- Wang, C., Chen, H., Zhu, X., Xiao, Z., Zhang, K., & Zhang, X. (2017). An improved polymeric sponge replication method for biomedical porous titanium scaffolds. *Materials Science and Engineering*, 70, 1192–1199.



- Wang, J., Zhang, J., Zhong, H., Wang, H., Ma, K., & Pan, L. (2020). Effect of support morphology and size of nickel metal ions on hydrogen production from methane steam reforming. *Chemical Physics Letters*, 746, 137291.
- Wen, Z. H., Han, Y. S., Liang, L., & Li, J. B. (2008). Preparation of porous ceramics with controllable pore sizes in an easy and low-cost way. *Materials Characterization*, 59, 1335–1338.
- Wichianrat, E., Boonyongmaneerat, Y., & Asavavisithchai, S. (2012). Microstructural examination and mechanical properties of replicated aluminium composite foams. *Trans. Nonferrous Met. Soc. China*, 22, 1674–1679.
- Wu, H., La Parola, V., Pantaleo, G., Puleo, F., Venezia, A., & Liotta, L. (2013). Ni-based catalysts for low temperature methane steam reforming: Recent results on Ni-Au and comparison with other bi-metallic systems. *Catalysts*, 3(2), 563–583.
- Xu, C., Wang, S., Flodström, K., Mao, X., & Guo, J. (2010). Cellular silica-based ceramics prepared by direct foaming at high temperature. *Ceramics International*, 36(3), 923–927.
- Yang, X. G., Duan, D. L., Zhang, X., Jiang, S. L., Li, S., & Zhang, H. C. (2019). Impact Behavior of Polyetheretherketone/Nickel Foam Co-continuous Composites. *Journal of Materials Engineering and Performance*, 28(10), 6380–6390.
- Yeh, S. K., Hsieh, C. C., Chang, H. C., Yen, C. C. C., & Chang, Y. C. (2015). Synergistic effect of coupling agents and fiber treatments on mechanical properties and moisture absorption of polypropylene–rice husk composites and their foam. *Composites Part A: Applied Science and Manufacturing*, 68, 313–322.
- Yokota, T., Takahata, Y., Katsuyama, T., & Matsuda, Y. (2001). A new technique for preparing ceramics for catalyst support exhibiting high porosity and high heat resistance. *Catalysis Today*, 69 (1–4), 11–15.



- Younes, M. M., Rahman, H. A. A., & Khattab, M. M. (2018). Utilization of rice husk ash and waste glass in the production of ternary blended cement mortar composites. *Journal of Building Engineering*, 20, 42–50.
- Yu, J., Wang, G., Tang, D., Qiu, Y., Sun, N., & Liu, W. (2018). A novel highly porous ceramic foam with efficient thermal insulation and high temperature resistance properties fabricated by gel-casting process. *IOP Conf. Series: Earth and Environmental Science*, 108, 022043.
- Zainal, N. S., Mohamad, Z., Mustapa, M. S., Badarulzaman, N. A., & Zulkifli, A. Z. (2019). The ability of crystalline and amorphous silica from rice husk ash to perform quality hardness for ceramic water filtration membrane. *International Journal of Integrated Engineering*, 11(5), 229–235.
- Zhang, L., Zhang, G., Lu, J., & Liang, H. (2013). Preparation and Characterization of Carboxymethyl Cellulose/Polyvinyl Alcohol Blend Film as a Potential Coating Material. *Polymer - Plastics Technology and Engineering*, 52(2), 163–167.
- Zhang, Y., Wang, W., Wang, Z., Zhou, X., Wang, Z., & Liu, C. J. (2015). Steam reforming of methane over Ni/SiO₂ catalyst with enhanced coke resistance at low steam to methane ratio. *Catalysis Today*, 256, 130–136.
- Zhao, J., Shimai, S., Zhou, G., Zhang, J., & Wang, S. (2017). Ceramic foams shaped by oppositely charged dispersant and surfactant. *Colloids and Surfaces A*, 537, 210–216.
- Zhao, L., Zhao, M., Li, N., Yan, H., & Zhang, J. (2010). Microstructure of nickel foam/Mg double interpenetrating composites. *Transactions of Nonferrous Metals Society of China*, 20(09497), s463–s466.
- Zheng, Q., Wang, Y., & Zhu, J. (2017). Nanoscale phase-change materials and devices. *Journal of Physics D: Applied Physics*, 50, 243002.
- Zhou, M., Ge, X., Wang, H., Chen, L., & Chen, X. (2017). Effect of the CaO content and decomposition of calcium-containing minerals on properties and microstructure of ceramic foams from fly ash. *Ceramics International*, 43, 9451–9457.



Zulkifli, N. S. C., Rahman, I. A., Mohamad, D., & Husein, A. (2013). A green sol–gel route for the synthesis of structurally controlled silica particles from rice husk for dental composite filler. *Ceramics International*, 39(4), 4559–4567.



PTTA UTHM
PERPUSTAKAAN TUNKU TUN AMINAH